Studies in Engineering Mechanics

Report Number 31

AN INVESTIGATION OF THE PARAMETRIC RESONANCE OF RECTANGULAR PLATES REINFORCED WITH CLOSELY SPACED STIFFENERS

by

Roger C. Duffield

and

Nicholas Willems

August, 1968

CRES

THE UNIVERSITY OF KANSAS • CENTER FOR RESEARCH INC
ENGINEERING SCIENCE DIVISION • LAWRENCE, KANSAS

STUDIES IN ENGINEERING MECHANICS
REPORT NUMBER 31

AN INVESTIGATION OF THE PARAMETRIC RESONANCE OF RECTANGULAR PLATES REINFORCED WITH CLOSELY SPACED STIFFENERS

by

Roger C. Duffield

and

Nicholas Willems

The University of Kansas

Center for Research in Engineering Science

Lawrence, Kansas

ACKNOWLEDGEMENTS

NGL-17-002-001

The writers wish to acknowledge the support from NASA under grant ~~NsG-298~~ which made this investigation possible. Thanks are expressed to the University of Kansas Center for Research, Inc., Engineering Science Division, and to the University of Kansas Computation Center for their administrative and technical assistance. In addition, thanks are due to the Computer Research Center of the University of Missouri - Columbia for allowing the use of their computer in completing this project.*

---

*This report represents a portion of the results of the Ph.D. thesis by Roger C. Duffield, Assistant Professor of Mechanical and Aerospace Engineering at the University of Missouri - Columbia, under the supervision of Dr. Nicholas Willems, Professor of Civil Engineering at the University of Kansas.

TABLE OF CONTENTS

LIST OF FIGURES

LIST OF TABLES
(Appendix)

NOTATION

A_r	Cross-sectional area of a rib
A_s	Cross-sectional area of a stringer
a	Length of plate in the x-direction
b	Length of plate in the y-direction
D	Flexural rigidity of the plate = $E_t{}^3/12(1-\nu^2)$
D_x	Orthotropic Rigidity constant = $D + (E_r I_r/d)$
Dy	Orthotropic rigidity constant = $D + (E_s I_s/l)$
d	Distance between uniformly spaced ribs
E	Modulus of elasticity for the plate
E_r	Modulus of elasticity for a rib
E_s	Modulus of elasticity for a stringer
$G_r J_r$	Torsional rigidity of a rib
$G_s J_s$	Torsional rigidity of a stringer
G_r	Shear modulus of elasticity of a rib
G_s	Shear modulus of elasticity of a stringer
H	Orthotropic rigidity constant = D
h	Plate thickness
J_s	Bending rigidity parameter for a stringer = $E_s I_s/aD$
l	Distance between uniformly spaced stringers
M	Mass parameter for the plate = $a^4 \rho_p h/4\pi^4 D$
$(N_{xo})cr$	Critical in-plane force acting on the plate in the x-direction
N_{xo}	Static in-plane force acting on the plate in the x-direction

N_{xt}	Variable in-plane force acting on the plate in the x-direction
N_x	Total in-plane force acting on the plate in the x-direction
N_x^*	In-plane force acting on the orthotropic plate in the x-direction = $N_x + (P_r/d)$
N_{yo}	Static in-plane force acting on the plate in the y-direction
N_{yt}	Variable in-plane force acting on the plate in the y-direction
N_y	Total in-plane force acting of the plate in the y-direction
N_y^*	In-plane force acting on the orthotropic plate in the y-direction = $N_y + (P_s/l)$
P_r	Axial force acting on a rib
P_s	Axial force acting on a stringer
T	Kinetic energy of the stiffened plate
t	Time
V	Potential energy of the stiffened plate
u(x,y,z,t)	Deflection at (x,y) in the x-direction
v(x,y,z,t)	Deflection at (x,y) in the y-direction
w(x,y,z,t)	Deflection at (x,y) in the z-direction
x,y,z	Cartesian coordinates (z out of the middle-surface of the plate)
α_{cr}	Critical buckling parameter = $b^2 N_{xcr}/\pi^2 D$
$\bar{\alpha}$	Static in-plane load parameter = $b^2 N_{xo}/\pi^2 D$
α'	Variable in-plane load parameter = $b^2 N_{xt}/\pi^2 D$
β	Aspect ratio = a/b
γ	Frequency parameter = $\theta^2/4\Omega^2$
θ	Frequency of the in-plane loading

λ_s	Stringer parameter = A_s/ah
ν	Poisson's ratio for the plate
ρ_p	Mass density per unit volume of the plate
ρ_r	Mass density per unit volume of a rib
ρ_s	Mass density per unit volume of a stringer
Ω	Natural frequency
$[\ ]$	mxn matrix
$\{\ \}$	Column matrix

1. INTRODUCTION

1.1 Objective of the Investigation

The object of this investigation is to determine theoretically the boundaries of the regions of parametric resonance of a simply supported stiffened rectangular plate with closely spaced stiffeners of uniform size subjected to periodic in-plane boundary forces. The theory is developed so as to apply to plates reinforced by either or both longitudinal and transverse stiffeners. The effects of torsional rigidity and rotary inertia of the stiffeners are also taken into account. Finally, the effects of size and location of the stiffeners on the boundaries of the regions of parametric resonance are studied.

1.2 History

Parametric instability mainly concerns the study of the response of a mechanical or elastic system to certain types of periodic loads. The term "parametric instability" stems from the fact that the time-dependent load appears in the coefficients (parameters) of the differential equation of motion of the system.

The problem of parametric instability has been studied by several investigators (1, 2, 3, 4). A complete history of the parametric instability of elastic systems through 1951 is given by Beilin and Dzhanelidze (5).* A more recent review of the history is given by Evan-Iwanowski (6,7).

An article by Beliaev (8), published in 1924, is considered to be the first analysis of parametric instability of a structure. He studied the parametric response of a simply-supported beam subjected to periodic axial loads of the type $P(t) = P_o + P_t \cos\Theta t$.

The nonlinear problem associated with the parametric response of an elastic column was studied by Weidenhammer (9, 10), by Bolotin (11, 12), and by Grybos (13). Bolotin and Grybos not only studied the nonlinear effects in the principal region of instability, but also the higher order parametric instability regions.

---

*Numbers in parenthesis designate references listed in the Bibliography.

Experimental verification of the principal region of parametric resonance reported by Beliaev and others was first obtained by Utida and Sezawa (14). Bolotin (11), verified the existence of the principal region of parametric resonance and he also verified the behavior of the column within the region of instability. The most extensive experimental investigation of the boundaries of the principal region was performed by Somerset (15,116), in 1964, who was the first to take P_o, P_1 and of the axial load, $P(t) = P_o + P_1 \cos \Theta t$, to be independent variables.

The research in the area of parametric instability of plate structures is not as extensive as for columns. The first investigation on rectangular plates was done in 1936 by Einaudi (17).

Bolotin (18, 19), was the first to investigate nonlinear problems of parametric response of a rectangular elastic plate. Somerset (20, 21, 22) in 1965 reinvestigated Bolotin's nonlinear problems, and his investigation is mainly concerned with an experimental study of the nonlinear problem. This experimental study is the only experimental work that has been performed in the area of plates prior to the work done in the investigation presented here.

Vu and Lai (23, 24), 1966, investigated the linear and nonlinear problems of parametric response of a sandwich plate. Ambratsumyan and Gnuni (25, 26), 1961, studied the linear and nonlinear problem for an infinitely long three layered plate and took into account linear damping. The nonlinear problem for three layered plates was also studied by Schmidt (27) in 1965.

Research in the proximity of the area of parametric instability of stiffened plates was done by Ambratsumyan and Khachaturian (28, 29) in 1959 and 1960. They studied the vibrational and dynamic stability characteristics of rectangular anistropic plates using a theory not based on Kirchhoff's hypothesis.

1.3 Background Information

There are several mathematical models which can be used to represent a stiffened plate system. In this investigation, two different mathematical models are considered; which are:
(1) The plate and stiffeners each considered as discrete elements.
(2) The stiffened plate considered as an equivalent orthotropic plate.

The first mathematical model is an "exact" model. The parametric resonance of a rectangular plate reinforced with both longitudinal and transverse stiffeners using the "exact" model was studied by Duffield and Willems (30). The second mathematical model requires some justification for its use since it is an approximation. An orthotropic structure has mechanical properties which possess three orthogonal planes of elastic symmetry at each point. Examination of a stiffened plate shows that its overall mechanical properties are different in different directions.

Gerard studied the orthotropic model for stability problems and states (31) that "orthotropic theory may be used for compressed plates with three or more stiffeners, for plates in shear with any number of longitudinal stiffeners and for transversely stiffened plates for relatively small or large values of EI/bD" (bending rigidity parameter). Gerard's statement for compressed plates is based mainly on the results of Seide (32). Seide's results show that the error in the stability parameter using the orthotropic plate theory for stiffened plates with three stiffeners is of the order of ten percent. The error increases for small values of the bending rigidity parameter of the stiffeners. The error decreases, however, with an increasing number of stiffeners.

Using an "exact" model, Wah (33) studied the vibrational characteristic of a stiffened plate and compared his results with those of an orthotropic plate. His study reveals closer agreement between the "exact" model composed of three stiffeners and the orthotropic model, as compared to the stability case. However, only one parameter for bending rigidity was studied.

In the investigation, several assumptions are made when the stiffened plate is treated as consisting of discrete elements. When the ribs and stringers are of a uniform size respectively and are closely spaced, the stiffened plate can be considered as an equivalent orthotropic plate. The problem of treating the stiffened plate as an equivalent orthotropic plate lies in the determination of the equivalent orthotropic rigidity constants for the plate. There are both experimental and theoretical methods available for the determination of the rigidity constants.

Procedures to determine the rigidity constants experimentally were devised by Hoffman and his coworkers (34, 35, 36) and Beckett (37). The trouble with the experimental determination of the rigidity constants is that the plate must first be designed with no knowledge of the magnitude of the rigidity constants and then redesigned after the rigidity constants are found. Huffington (38) devised a theoretical method for the determination of the rigidity constants of a stiffened plate with only closely spaced ribs. He based the equivalence of the real system and the orthotropic system upon the equality of their strain energies. An experimental verification of his results showed good agreement. Another approach used by several investigators (37, 38) is to average or "smear out" the elastic and geometric properties of the stiffener over the stiffener spacing. The advantage of the theoretical approach is that the obtained equivalent rigidity constants are expressed in terms of the stiffened plates elastic and geometric properties.

2. THEORETICAL ANALYSIS

2.1 Assumption

The investigation presented in this analysis is limited to a dynamic system so constructed that the stiffeners are attached to the plate in such a manner that the middle-surface of the stiffeners coincides with the middle-surface of the plate. It is assumed that the assumptions of both the classical plate and beam theories hold for this system. It is also assumed that:

(1) The plate, ribs and stringers are fabricated from isotropic materials
(2) The ribs and stringers respectively all have the same elastic and geometric properties
(3) A perfect bond exists between the plate and the stiffeners

In this investigation in the in-plane loading is taken to be periodic in nature. The magnitude of the in-plane loading, applied at the boundaries of the system, will propagate at the speed of the longitudinal frequency of the system. If the frequency of the periodic in-plane boundary loading is taken to be considerably below that of the longitudinal frequency, it is reasonable to assume that the magnitude of the loading is independent of the space coordinates of the system. This implies that the whole system instantaneously senses the magnitude of the loading and that the in-plane inertia effects due to the periodic in-plane boundary loading are negligible.

2.2 Basic Energy Expressions

The kinetic and potential energies of the equivalent orthotropic plate can be obtained directly from the kinetic and potential energies of the stiffened plate when it is considered as a discrete element model by using the "averaging" or "smearing out" technique. The total potential energy of the discrete element model is the sum of the strain and external potential energies. In this investigation the external in-plane forces are limited to those which are expressable in terms of a time-dependent potential. Thus, for the discrete system the total potential energy (39) is

$$V = \frac{D}{2}\int_0^a\int_0^b \left\{\left(\frac{\partial^2 W}{\partial X^2} + \frac{\partial^2 W}{\partial Y^2}\right)^2 - 2(1-\nu)\left[\frac{\partial^2 W}{\partial X^2}\frac{\partial^2 W}{\partial Y^2} - \left(\frac{\partial^2 W}{\partial X\partial Y}\right)^2\right]\right\} dX\,dY -$$

$$-\frac{1}{2}\int_0^a\int_0^b \left[N_X\left(\frac{\partial W}{\partial X}\right)^2 + N_Y\left(\frac{\partial W}{\partial Y}\right)^2\right] dX\,dY + \sum_{i=1}^{R}\frac{E_{ri}I_{ri}}{2}\int_0^a \left(\frac{\partial^2 W}{\partial X^2}\right)^2_{Y=Y_i} dX +$$

$$+\sum_{K=1}^{P}\frac{E_{sK}I_{sK}}{2}\int_0^b \left(\frac{\partial^2 W}{\partial Y^2}\right)^2_{X=X_K} dY + \sum_{i=1}^{R}\frac{G_{ri}J_{ri}}{2}\int_0^a \left(\frac{\partial^2 W}{\partial X\partial Y}\right)^2_{Y=Y_i} dX +$$

$$+\sum_{k=1}^{P}\frac{G_{sk}J_{sk}}{2}\int_0^b\left(\frac{\partial^2 w}{\partial x\partial y}\right)^2_{x=x_k}dy-\sum_{i=1}^{R}\frac{P_{ri}}{2}\int_0^a\left(\frac{\partial w}{\partial x}\right)_{y=y_i}dx-\sum_{k=1}^{P}\frac{P_{sk}}{2}\int_0^b\left(\frac{\partial w}{\partial y}\right)_{x=x_k}dy \quad \text{--- (1)}$$

in which E_{ri} and E_{sk} are the moduli of elasticity, I_{ri} and I_{sk} are the moments of inertia, and $G_{ri}J_{ri}$ and $G_{sk}J_{sk}$ are the torsional rigidities at the i^{th} rib and k^{th} stringer respectively, see Fig. 1. (See notation page for the definition of the remaining symbols in Eq. (1).) The effect of the torsional rigidity of the stiffeners is included in the determination of the total potential energy, Eq. (1), for the dynamic system. The averaging or "smearing out" of the effects of the stiffeners results in the following equation for the total potential energy, which is

$$V=\frac{1}{2}\int_0^a\int_0^b\Bigg[\left(D+\frac{E_rI_r}{d}\right)\left(\frac{\partial^2 w}{\partial x^2}\right)^2+\left(D+\frac{E_sI_s}{l}\right)\left(\frac{\partial^2 w}{\partial y^2}\right)^2+2D\nu\,\frac{\partial^2 w}{\partial x^2}\,\frac{\partial^2 w}{\partial y^2}+$$

$$+\left(2D(1-\nu)+\frac{G_rJ_r}{d}+\frac{G_sJ_s}{l}\right)\left(\frac{\partial^2 w}{\partial x\partial y}\right)^2-\left(\frac{P_r}{d}+N_x\right)\left(\frac{\partial w}{\partial x}\right)^2-$$

$$-\left(\frac{P_s}{l}+N_y\right)\left(\frac{\partial w}{\partial y}\right)^2\Bigg]dx\,dy \quad \text{--- (2)}$$

in which d is the spacing between the centers of the ribs and l is the spacing between the centers of the stringers.

The total kinetic energy of the discrete system is the sum of the kinetic energies of the plate and the stiffeners (39). Thus the total kinetic energy is

$$T=\frac{1}{2}\int_0^a\int_0^b\left[\rho_p h\left(\frac{\partial w}{\partial t}\right)^2+I_{px}\left(\frac{\partial^2 w}{\partial y\partial t}\right)^2+I_{py}\left(\frac{\partial^2 w}{\partial x\partial t}\right)^2\right]dx\,dy+$$

$$+\frac{1}{2}\sum_{i=1}^{R}\int_0^a\left[\rho_{ri}A_{ri}\left(\frac{\partial w}{\partial t}\right)^2_{y=y_i}+I'_{ri}\left(\frac{\partial^2 w}{\partial x\partial t}\right)^2_{y=y_i}+I''_{ri}\left(\frac{\partial^2 w}{\partial y\partial t}\right)^2_{y=y_i}\right]dx+$$

$$+\frac{1}{2}\sum_{k=1}^{P}\int_0^b\left[\rho_{sk}A_{sk}\left(\frac{\partial w}{\partial t}\right)^2_{x=x_k}+I'_{sk}\left(\frac{\partial^2 w}{\partial y\partial t}\right)^2_{x=x_k}+I''_{sk}\left(\frac{\partial^2 w}{\partial x\partial t}\right)^2_{x=x_k}\right]dy \quad \text{--- (3)}$$

in which I_{px} and I_{py} are the mass moments of inertia per unit area of a small characteristic element of the plate about axes x' and y' which pass through the center of gravity of the element and which are parallel to the x and y axes respectively, I'_{ri}, I''_{ri} and I'_{sk} are the mass moments of inertia about the neutral (') and longitudinal (") axes for the i^{th} rib and k^{th} stringer respectively. The effect of rotatory inertia is

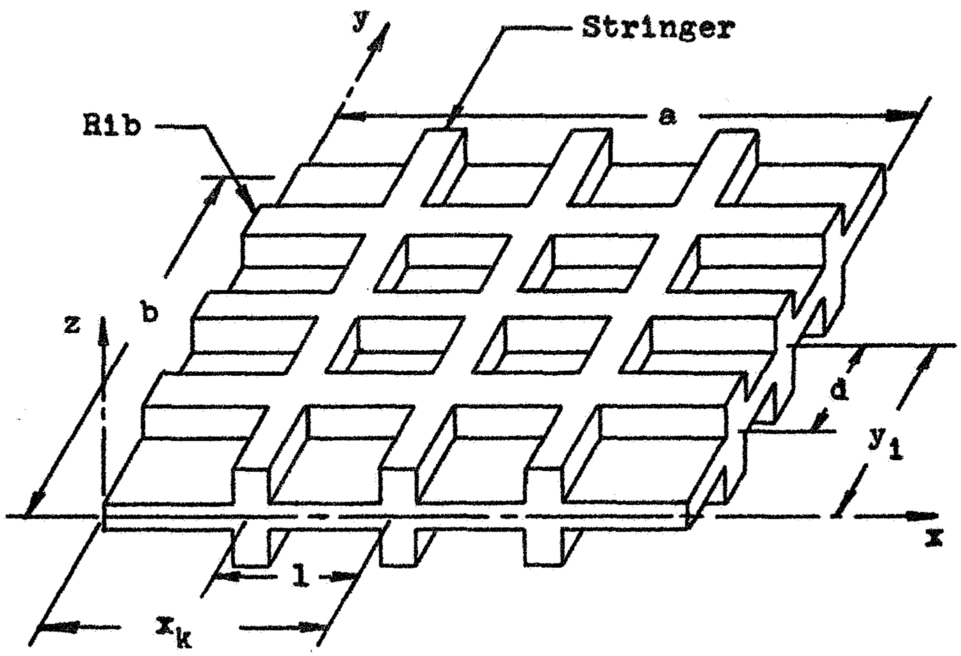

Fig. 1 An Equivalent Orthotropic Plate

included in the determination of the kinetic energy, Eq. (3), for the dynamic system under consideration. When the effect of the stiffeners is averaged or "smeared out" the expression for the kinetic energy takes the form

$$T=\frac{1}{2}\int_0^a\int_0^b\Big[\Big(\rho_p h+\frac{\rho_r A_r}{d}+\frac{\rho_s A_s}{\ell}\Big)\Big(\frac{\partial w}{\partial t}\Big)^2+\Big(I_{px}+\frac{I''_r}{d}+\frac{I'_s}{\ell}\Big)\Big(\frac{\partial^2 w}{\partial y\,\partial t}\Big)^2+$$
$$+\Big(I_{py}+\frac{I'_r}{d}+\frac{I''_s}{\ell}\Big)\Big(\frac{\partial^2 w}{\partial x\,\partial t}\Big)^2\Big]\,dx\,dy \qquad \text{--- (4)}$$

2.3 Hamilton's Principle

The dynamic behavior of a continuous system can be formulated in terms of Hamilton's principle. Hamilton's principle is essential to this investigation in that it is the starting point for the determination of the equations of motion and boundary conditions for the dynamic systems under consideration. The mathematical statement of Hamilton's principle for a conservative system is

$$\delta A=0 \qquad \text{--- (5)}$$

in which

$$A=\int_{t_1}^{t_2} L\,dt \qquad \text{--- (6)}$$

and

$$L=T-V \qquad \text{--- (7)}$$

in which T is the kinetic energy of the system, V is the potential work energy of the noninertial forces acting on the system, and t_1 and t_2 are two instants of time. The expression A is generally referred to as the "action integral" and L is known as the "Lagrangian function". The formulation of the dynamic behavior for the systems under investigation in terms of Hamilton's principle can be obtained by the substitution of Eqs. (2) and (4) into Eq. (5), which results in

$$\delta A=\int_{t_1}^{t_2}\int_0^a\int_0^b\frac{1}{2}\Big[\Big(\rho_p h+\frac{\rho_r A_r}{d}+\frac{\rho_s A_s}{\ell}\Big)\Big(\frac{\partial w}{\partial t}\Big)^2+\Big(I_{px}+\frac{I''_r}{d}+\frac{I'_s}{\ell}\Big)\cdot$$
$$\cdot\Big(\frac{\partial^2 w}{\partial t\,\partial y}\Big)^2+\Big(I_{py}+\frac{I'_r}{d}+\frac{I''_s}{\ell}\Big)\Big(\frac{\partial^2 w}{\partial t\,\partial x}\Big)^2-\Big(D+\frac{E_r I_r}{d}\Big)\Big(\frac{\partial^2 w}{\partial x^2}\Big)^2-$$
$$-\Big(D+\frac{E_s I_s}{\ell}\Big)\Big(\frac{\partial^2 w}{\partial y^2}\Big)^2-2D\nu\,\frac{\partial^2 w}{\partial y^2}\,\frac{\partial^2 w}{\partial x^2}-\Big(2D(1-\nu)+\frac{G_r J_r}{d}+\frac{G_s J_s}{\ell}\Big)\cdot$$
$$\cdot\Big(\frac{\partial^2 w}{\partial x\,\partial y}\Big)^2+\Big(\frac{P_r}{d}+N_x\Big)\Big(\frac{\partial w}{\partial x}\Big)^2+\Big(\frac{P_s}{\ell}+N_y\Big)\Big(\frac{\partial w}{\partial y}\Big)^2\Big]\,dx\,dy=0 \qquad \text{--- (8)}$$

2.4 Equations of Motion and Boundary Conditions

When the behavior of the system is formulated in terms of Hamilton's principle, the problem reduces to the determination of the necessary and sufficient conditions on the function $w(x,y,t)$ such that the integral A of Eq. (8) is stationary. The determination of these conditions requires the use of calculus of variations, see references (40, 41, 42, 43). The necessary conditions which the function w must satisfy generally take the form of differential equations with admissible boundary conditions. The sufficient conditions are mathematically more difficult to determine. However, Hamilton's principle, based on physical considerations, serves as the sufficient condition.

In this study, the function $w(x,y,t)$, with continuous fourth order partial derivatives in R, is taken to be the function which makes the integral A in Eq. (8) stationary. A comparison function in the neighborhood of $w(x,y,t)$ can be constructed of the form

$$\overline{w}(x,y,t) = w(x,y,t) + \epsilon\eta(x,y,t) \qquad \text{--- (9)}$$

in which ϵ is a small but otherwise arbitrary scalar and $\eta(x,y,t)$ is an arbitrary function with continuous fourth order partial derivatives which vanishes at the end points $t = t_0$ and $t = t_1$. This last condition on η is required because of the formulation of Hamilton's principle. Since $w(x,y,t)$ gives the integral A a stationary value, then this implies that for $\bar{w}(x,y,t)$

$$A(\overline{w}) \geq A(w) \qquad \text{--- (10)}$$

Equation (10) reveals that the integral $A(w+\epsilon\eta)$, as a function of ϵ, takes on a stationary value when $\epsilon = 0$. Therefore, the necessary condition for $A(w+\epsilon\eta)$ to have a stationary value at $\epsilon = 0$ is

$$\left.\frac{dA(\epsilon)}{d\epsilon}\right|_{\epsilon=0} = 0 \qquad \text{--- (11)}$$

The replacement of $w(x,y,t)$ in Eq. (8) by the comparison function given by Eq. (9) and the corresponding application of Eq. (11) to Eq. (8) gives

$$\left.\frac{dA}{d\epsilon}\right|_{\epsilon=0} = \int_{t_1}^{t_2}\int_0^a\int_0^b \Big[\Big(\rho_p h + \frac{\rho_r A_r}{d} + \frac{\rho_s A_s}{\ell}\Big)\frac{\partial w}{\partial t}\frac{\partial \eta}{\partial t} + \Big(I_{px} + \frac{I_r''}{d}$$

$$+ \frac{I_s'}{\ell}\Big)\frac{\partial^2 w}{\partial y\partial t}\frac{\partial^2 \eta}{\partial y\partial t} + \Big(I_{py} + \frac{I_r'}{d} + \frac{I_s''}{\ell}\Big)\frac{\partial^2 w}{\partial x\partial t}\frac{\partial^2 \eta}{\partial x\partial t} -$$

$$-\Big(D + \frac{E_r I_r}{d}\Big)\frac{\partial^2 w}{\partial x^2}\frac{\partial^2 \eta}{\partial x^2} - \Big(D + \frac{E_s I_s}{\ell}\Big)\frac{\partial^2 w}{\partial y^2}\frac{\partial^2 \eta}{\partial y^2} - D\nu\frac{\partial^2 w}{\partial x^2}\frac{\partial^2 \eta}{\partial y^2} -$$

$$-D\nu\frac{\partial^2 w}{\partial x^2}\frac{\partial^2 \eta}{\partial y^2} - \Big(2D(1-\nu) + \frac{G_r J_r}{d} + \frac{G_s J_s}{\ell}\Big)\frac{\partial^2 w}{\partial x\partial y}\frac{\partial^2 \eta}{\partial x\partial y} +$$

$$+\Big(\frac{P_r}{d} + N_x\Big)\frac{\partial w}{\partial x}\frac{\partial \eta}{\partial x} + \Big(\frac{P_s}{\ell} + N_y\Big)\frac{\partial w}{\partial y}\frac{\partial \eta}{\partial y}\Big]dx\,dy\,dt = 0 \quad \text{--- (12)}$$

After considerable manipulation and applying the technique of integration by parts or the divergence theorem

$$\int_R \frac{\partial u}{\partial x_i}\, dx_1 \text{\_\_\_\_} dx_q = \int_S u\,\frac{\partial x_i}{\partial n}\, ds \quad \text{--- (13)}$$

in which u is a continuous function, x_i is the i^{th} coordinate of a set of q coordinates, S is the surface or contour of the region R, and n is the normal to S, Eq. (12) takes the form

$$\int_{t_1}^{t_2}\int_0^a\int_0^b \Big[-\Big(\rho_p h + \frac{\rho_r A_r}{d} + \frac{\rho_s A_s}{\ell}\Big)\frac{\partial^2 w}{\partial t^2} + \Big(I_{px} + \frac{I_r''}{d} + \frac{I_s'}{\ell}\Big)\frac{\partial^4 w}{\partial y^2\partial t^2} +$$

$$+\Big(I_{py} + \frac{I_r'}{d} + \frac{I_s''}{\ell}\Big)\frac{\partial^4 w}{\partial x^2\partial t^2} - \Big(D + \frac{E_r I_r}{d}\Big)\frac{\partial^4 w}{\partial x^4} - \Big(D + \frac{E_s I_s}{\ell}\Big)\frac{\partial^4 w}{\partial y^4} -$$

$$-2D\nu\frac{\partial^4 w}{\partial x^2\partial y^2} - \Big(2D(1-\nu) + \frac{G_r J_r}{d} + \frac{G_s J_s}{\ell}\Big)\frac{\partial^4 w}{\partial x^2\partial y^2} - \Big(\frac{P_r}{d} + N_x\Big)\frac{\partial^2 w}{\partial x^2} -$$

$$-\Big(\frac{P_s}{\ell} + N_y\Big)\frac{\partial^2 w}{\partial y^2}\Big]\eta\, dx\,dy\,dt + \int_{t_1}^{t_2}\oint_S \Big\{\Big[-\Big(I_{px} + \frac{I_r''}{d} + \frac{I_s'}{\ell}\Big)\frac{\partial^3 w}{\partial y\partial t^2} +$$

$$+\Big(D + \frac{E_s I_s}{\ell}\Big)\frac{\partial^3 w}{\partial y^3} + D\nu\frac{\partial^3 w}{\partial x^2\partial y} + \Big(2D(1-\nu) + \frac{G_r J_r}{d} + \frac{G_s J_s}{\ell}\Big)\frac{\partial^3 w}{\partial x^2\partial y} +$$

$$+\Big(\frac{P_s}{\ell} + N_y\Big)\frac{\partial w}{\partial y}\Big]\frac{\partial y}{\partial n}\eta + \Big[-\Big(I_{py} + \frac{I_r'}{d} + \frac{I_s''}{\ell}\Big)\frac{\partial^3 w}{\partial x\partial y^2} + D\nu\frac{\partial^3 w}{\partial y^2\partial x} +$$

$$+\left(D+\frac{E_rI_r}{d}\right)\frac{\partial^3 w}{\partial x^3}+\left(2D(1-\nu)+\frac{G_rJ_r}{d}+\frac{G_sJ_s}{\ell}\right)\frac{\partial^3 w}{\partial x\partial y^2}+\left(\frac{P_r}{\ell}+N_x\right)\cdot$$

$$\cdot\left.\frac{\partial w}{\partial x}\right]\frac{\partial x}{\partial n}\eta+\left[-\left(D+\frac{E_sI_s}{\ell}\right)\frac{\partial^2 w}{\partial y^2}-D\nu\frac{\partial^2 w}{\partial x^2}\right]\frac{\partial y}{\partial n}\frac{\partial\eta}{\partial y}+\left[-\left(\frac{D+E_rI_r}{d}\right)-\right.$$

$$\left.\left.-D\nu\frac{\partial^2 w}{\partial y^2}\right]\frac{\partial x}{\partial n}\frac{\partial\eta}{\partial x}\right\}ds\,dt-\left(2D(1-\nu)+\frac{G_sJ_s}{\ell}+\frac{G_rJ_r}{d}\right)\int_{t_1}^{t_2}\left(\frac{\partial^2 w}{\partial x\partial y}\right)^2\eta\Big|_{y=b}\Big|_0^a dt+$$

$$+\left(2D(1-\nu)+\frac{G_sJ_s}{\ell}+\frac{G_rJ_r}{d}\right)\int_{t_1}^{t_2}\left(\frac{\partial^2 w}{\partial x\partial y}\right)^2\eta\Big|_{y=0}\Big|_0^a dt=0 \qquad \text{--- (14)}$$

The application of the "fundamental lemma of the calculus of variations" to Eq. (14) together with the knowledge that η is an arbitrary function yields a partial differential equation with admissible boundary conditions that constitute the necessary conditions on w(x,y,t) for δA to be stationary. The partial differential equation that results from Eq. (14) is

$$\left(\rho_p h+\frac{\rho_r A_r}{d}+\frac{\rho_s A_s}{\ell}\right)\frac{\partial^2 w}{\partial t^2}-\left(I_{px}+\frac{I_r''}{d}+\frac{I_s'}{\ell}\right)\frac{\partial^4 w}{\partial y^2\partial t^2}-$$

$$-\left(I_{py}+\frac{I_r'}{d}+\frac{I_s''}{\ell}\right)\frac{\partial^4 w}{\partial x^2\partial t^2}+\left(D+\frac{E_rI_r}{d}\right)\frac{\partial^4 w}{\partial x^4}+\left(2D+\frac{G_rJ_r}{d}+\right.$$

$$\left.+\frac{G_sJ_s}{\ell}\right)\frac{\partial^4 w}{\partial x^2\partial y^2}+\left(D+\frac{E_sI_s}{\ell}\right)\frac{\partial^4 w}{\partial y^4}+\left(\frac{P_r}{d}+N_x\right)\frac{\partial^2 w}{\partial x^2}+$$

$$+\left(\frac{P_s}{\ell}+N_y\right)\frac{\partial^2 w}{\partial y^2}=0 \qquad \text{--- (15)}$$

The determination of the admissible boundary conditions from Eq. (14) for a rectangular region requires the application of the following relations $\partial x/\partial n = 0$ for n = y, $\partial x/\partial n = 1$ for n = x, $\partial y/\partial n = 0$ for n = x, and $\partial y/\partial n = 1$ for n = y. Thus, the boundary conditions for the edges of the plate parallel to the y-axis are:

$$D\left(\frac{\partial^3 w}{\partial x^3}+\nu\frac{\partial^3 w}{\partial x\partial y^2}\right)+\frac{E_rI_r}{d}\frac{\partial^3 w}{\partial x^3}+\left(\frac{G_p h^3}{3}+\frac{G_rJ_r}{d}+\frac{G_sJ_s}{\ell}\right)\frac{\partial^3 w}{\partial x\partial y^2}-$$

$$-\left(I_{py}+\frac{I_r'}{d}+\frac{I_s''}{\ell}\right)\frac{\partial^3 w}{\partial x\partial t^2}+\left(\frac{P_r}{d}+N_x\right)\frac{\partial w}{\partial x}=0 \qquad \text{--- (16)}$$

$$w \text{ prescribed} \rightarrow \eta=0 \qquad \text{--- (17)}$$

$$D\left(\frac{\partial^2 w}{\partial x^2}-\nu\frac{\partial^2 w}{\partial y^2}\right)+\frac{E_rI_r}{d}\frac{\partial^2 w}{\partial x^2}=0 \qquad \text{--- (18)}$$

$$\frac{\partial w}{\partial x}\text{ prescribed} \rightarrow \frac{\partial\eta}{\partial x}=0 \qquad \text{--- (19)}$$

in Eq. (16), G_p is the shearing modulus of elasticity for the plate. The boundary conditions for the edges of the plate parallel to the x-axis are:

$$D\left(\frac{\partial^3 w}{\partial y^3} + \nu \frac{\partial^3 w}{\partial y \partial x^2}\right) + \frac{E_s I_s}{l} \frac{\partial^3 w}{\partial y^3} + \left(\frac{G_p h^3}{3} + \frac{G_r J_r}{d} + \frac{G_s J_s}{l}\right) \frac{\partial^3 w}{\partial x^2 \partial y} -$$

$$-\left(I_{px} + \frac{I_r''}{d} + \frac{I_s''}{l}\right) \frac{\partial^3 w}{\partial y \partial t^2} + \left(\frac{P_s}{l} + N_y\right) \frac{\partial w}{\partial y} = 0 \qquad \text{--- (20)}$$

or

$$w \qquad \rightarrow \eta = 0 \qquad \text{--- (21)}$$

$$D\left(\frac{\partial^2 w}{\partial y^2} - \nu \frac{\partial^2 w}{\partial x^2}\right) + \frac{E_s I_s}{l} \frac{\partial^2 w}{\partial y^2} = 0 \qquad \text{--- (22)}$$

or

$$\frac{\partial w}{\partial y} \text{ prescribed} \rightarrow \frac{\partial \eta}{\partial y} = 0 \qquad \text{--- (23)}$$

At the corners of the rectangular plate the following conditions must be satisfied

$$\frac{\partial^2 w}{\partial x \partial y} = 0 \qquad \text{--- (24)}$$

in which w must be evaluated at the corner, or

$$w \text{ prescribed at the corners} \rightarrow \eta = 0 \qquad \text{--- (25)}$$

Equations (15) through (25) represent the necessary conditions $w(x,y,t)$ for $\delta A(w)$ to be stationary.

If the effect of torsional rigidity is neglected and if w is taken to be independent of time, then Eq. (15) reduces to the form

$$D_x \frac{\partial^4 w}{\partial x^4} + 2H \frac{\partial^4 w}{\partial x^2 \partial y^2} + D_y \frac{\partial^4 w}{\partial y^4} + N_x^* \frac{\partial^2 w}{\partial x^2} + N_y^* \frac{\partial^2 w}{\partial y^2} = 0 \qquad \text{--- (26)}$$

in which

$$D_x = D + \frac{E_r I_r}{d} \qquad \text{--- (27)}$$

$$D_y = D + \frac{E_s I_s}{\ell} \qquad \text{--- (28)}$$

$$H = D \qquad \text{--- (29)}$$

$$N_x^* = \frac{P_r}{d} + N_x \qquad \text{--- (30)}$$

and

$$N_y^* = \frac{P_s}{\ell} + N_y \qquad \text{--- (31)}$$

Equations (27) through (31) agree with the values of the orthotropic rigidity constants obtained by Huffington (36) for the limiting case of closely spaced ribs only. These same three equations also agree with the orthotropic rigidity constants proposed by Lechnitskii (44). Equation (26) represents the governing equation for the case of static stability of an orthotropic plate.

The substitution of Eqs. (27), (28), (30) and (31) into Eq. (15) along with the introduction of additional parameters yields

$$D_x \frac{\partial^4 w}{\partial x^4} + 2H \frac{\partial^4 w}{\partial x^2 \partial y^2} + D_y \frac{\partial^4 w}{\partial y^4} + M \frac{\partial^2 w}{\partial t^2} - M' \frac{\partial^4 w}{\partial y^2 \partial t^2} - M'' \frac{\partial^4 w}{\partial x^2 \partial t^2} +$$

$$+ N_x^* \frac{\partial^2 w}{\partial x^2} + N_y^* \frac{\partial^2 w}{\partial y^2} = 0 \qquad \text{--- (32)}$$

in which

$$M = \rho p h + \frac{\rho_r A_r}{d} + \frac{\rho_s A_s}{\ell} \quad \text{--- (33)}$$

$$M' = I_{px} + \frac{I_r''}{d} + \frac{I_s'}{\ell} \quad \text{--- (34)}$$

$$M'' = I_{py} + \frac{I_r'}{d} + \frac{I_s''}{\ell} \quad \text{--- (35)}$$

and

$$H = D + \frac{G_r J_r}{2d} + \frac{G_s J_s}{2\ell} \quad \text{--- (36)}$$

which replaces H in Eqs. (29). In terms of the parameters introduced above, the boundary conditions for the edges of the plate parallel to the y-axis take the form

$$D_x \frac{\partial^3 w}{\partial x^3} + (2H - \nu D) \frac{\partial^3 w}{\partial x \partial y^2} - M' \frac{\partial^3 w}{\partial x \partial t} + N_x^* \frac{\partial w}{\partial x} = 0 \quad \text{--- (37)}$$

or

$$w \text{ prescribed} \quad \text{--- (38)}$$

$$D_x \frac{\partial^2 w}{\partial x^2} - \nu D \frac{\partial^2 w}{\partial y^2} = 0 \quad \text{--- (39)}$$

or

$$\frac{\partial w}{\partial x} \text{ prescribed} \quad \text{--- (40)}$$

The boundary conditions for the edges of the stiffened plate parallel to the x-axis in term of the parameter given above are

$$D_y \frac{\partial^3 w}{\partial y^3} + (2H - \nu D) \frac{\partial^3 w}{\partial x^2 \partial y} - M'' \frac{\partial^3 w}{\partial y \partial t^2} - N_y^* \frac{\partial w}{\partial y} = 0 \qquad \text{--- (41)}$$

or

$$w \quad \text{prescribed} \qquad \text{--- (42)}$$

$$D_y \frac{\partial^2 w}{\partial y^2} - \nu D \frac{\partial^2 w}{\partial x^2} = 0 \qquad \text{--- (43)}$$

or

$$\frac{\partial w}{\partial y} \quad \text{prescribed} \qquad \text{--- (44)}$$

2.5 Solution of the Equation of Motion

This section is concerned with the determination of a solution of Eq. (32) for the case of a rectangular stiffened plate with simply-supported edges, see Fig. 2. The boundary conditions for the simple-supports can be found from the equations for the admissable boundary conditions, Eqs. (37) through (44). The boundary conditions for the contour of the stiffened rectangular plate are

$$w(x,y,t)\Big|_{x=0,a} = 0 \qquad \text{--- (45)}$$

$$\frac{\partial^2 w\ x,y,t}{\partial x^2}\Bigg|_{x=0,a} = 0 \qquad \text{--- (46)}$$

$$w(x,y,t)\Big|_{y=0,b} = 0 \qquad \text{--- (47)}$$

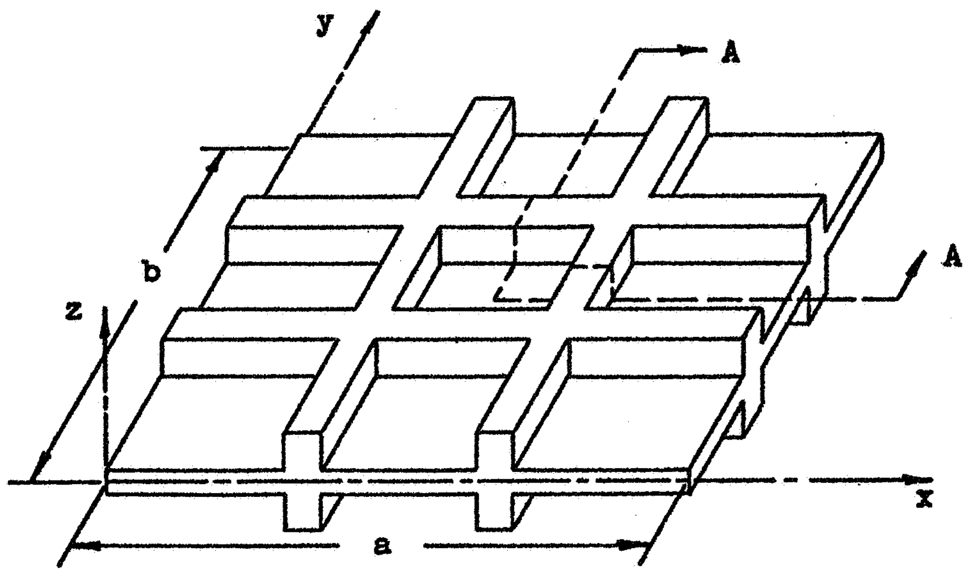

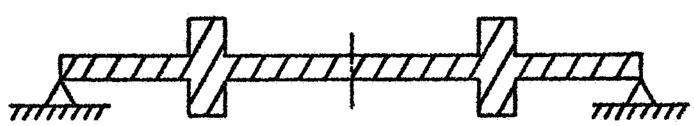

Section A-A

Fig. [illegible] A Simply-Supported Equivalent Orthotropic Plate

and

$$\left.\frac{\partial^2 W(x,y,t)}{\partial y^2}\right|_{y=0,b} = 0 \qquad \text{--- (48)}$$

The solution of Eq. (32) is sought in the form

$$W(x,y,t) = \sum_{m=1}^{\infty}\sum_{n=1}^{\infty} T_{mn}(t)\,\phi_{mn}(x,y) \qquad \text{--- (49)}$$

The functions $\phi_{mn}(x,y)$ must form a complete set of functions (45) over the rectangular region of the stiffened plate and they must also satisfy term by term the boundary conditions given by Eqs. (45) through (48). A set of functions, $\phi_{mn}(x,y)$, that are complete over the region of the stiffened plate $0 \leq x \leq a$ and $0 \leq y \leq b$ and which satisfy the simply supported boundary conditions are

$$\phi_{mn}(x,y) = \sin\frac{m\pi x}{a}\,\sin\frac{n\pi y}{b} \qquad \text{--- (50)}$$

The replacement of $\phi_{mn}(x,y)$ by Eq. (50) in Eq. (49) gives

$$W(x,y,t) = \sum_{m=1}^{\infty}\sum_{n=1}^{\infty} T_{mn}(t)\,\sin\frac{m\pi x}{a}\,\sin\frac{n\pi y}{b} \qquad \text{--- (51)}$$

The substitution of Eq. (51) into Eq. (32) gives

$$\sum_{m=1}^{\infty}\sum_{n=1}^{\infty}\left[\left(M + \frac{n^2\pi^2 M'}{b^2} + \frac{m^2\pi^2 M''}{a^2}\right)\ddot{T}_{mn} + \left(\frac{m^4\pi^4}{a^4}D_x + \frac{2n^2m^2\pi^4}{a^2b^2}H + \right.\right.$$

$$\left.\left. + \frac{n^4\pi^4}{b^4}D_y - \frac{m^2\pi}{a^2}N_x^* - \frac{n^2\pi^2}{b^2}N_y^*\right)T_{mn}\right]\sin\frac{m\pi x}{a}\,\sin\frac{n\pi y}{b} = 0$$

Since ϕ_{mn}, Eq. (50), represents a complete set of functions, the condition for linear independence

$$\sum_{m=1}^{\infty}\sum_{n=1}^{\infty} C_{mn}\,\phi_{mn} = 0 \qquad \text{--- (53)}$$

requires that each C_{mn} must be equal to zero. Equation (52) has the same form as Eq. (53) thus

$$\left(M + \frac{n^2\pi^2}{b^2}M' + \frac{m^2\pi^2 M''}{a^2}\right)\ddot{T}_{mn} + \left(\frac{m^4\pi^4}{a^4}D_x + \frac{2n^2m^2\pi^4}{a^2b^2}H + \right.$$

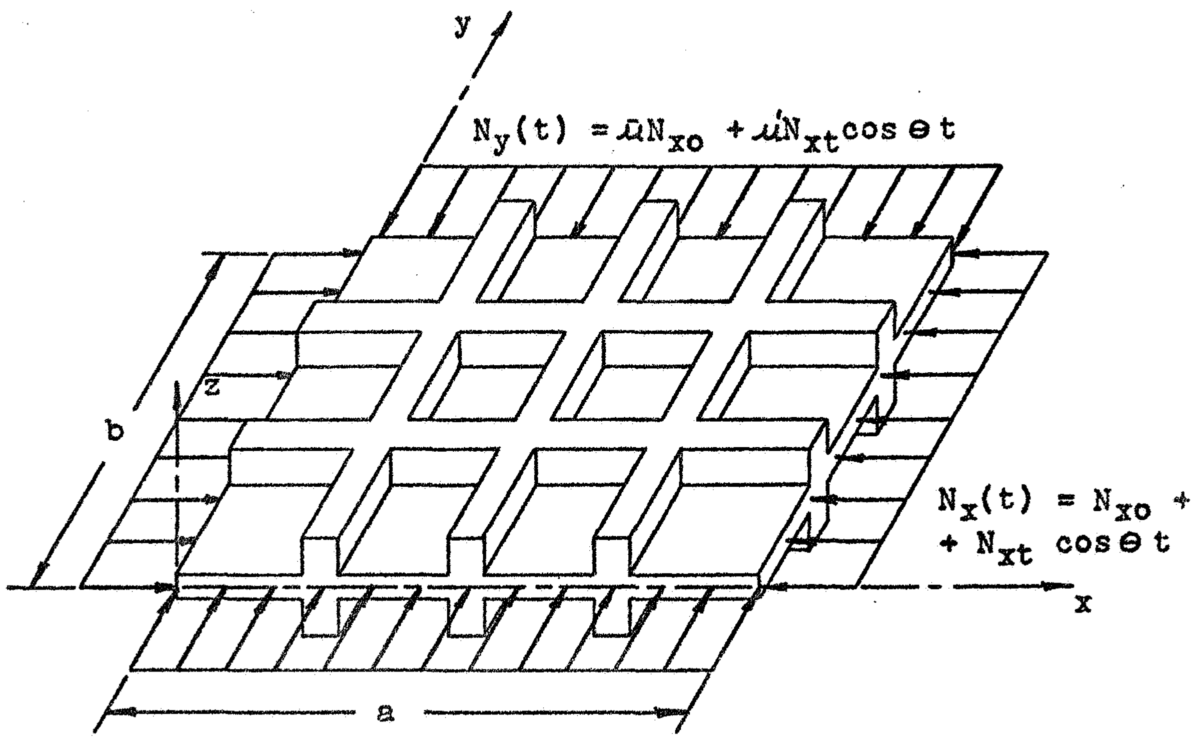

Fig. 3 An Equivalent Orthotropic Plate Subjected to Periodic In-plane Loading

$$+\frac{n^4\pi^4}{b^4}D_y-\frac{m^2\pi^2}{a^2}N_x^*-\frac{n^2\pi^2}{b^2}N_y^*\Big)T_{mn}=0 \qquad \text{--- (54)}$$

for m = 1,2,-- ∞, n = 1,2,-- ∞. Equation (54) is valid for any type of time-dependent in-plane edge forces acting on both the plate and stiffeners provided that the forces can be expressed in terms of time-dependent potentials.

In the investigation presented in this chapter only the effect of harmonic in-plane edge forces on the parametric instability of the stiffened plate is considered, see Fig. 3. The loading on the edge of the plate is

$$N_x(t)=N_{xo}+N_{xt}\cos\theta t \qquad \text{--- (55)}$$

and

$$N_y(t)=\bar{\mu}N_{xo}+\mu' N_{xt}\cos\theta t \qquad \text{--- (56)}$$

in which $\bar{\mu}$ and μ' are proportionality factors relating the magnitude of the static and variable components respectively of the in-plane loading on the plate in the x-direction to the corresponding components in the y-direction. The in-plane edge load on each rib and stringer respectively is the same and for the ribs has the form

$$P_r(t)=\frac{A_r}{h}\left[\bar{\nu}_r N_{xo}+\nu_r' N_{xt}\cos\theta t\right] \qquad \text{--- (57)}$$

and for the stringers

$$P_s(t)=\frac{A_s}{h}\left[\bar{\nu}_s\bar{\mu}N_{xo}+\nu_s'\mu' N_{xt}\cos\theta t\right] \qquad \text{--- (58)}$$

in which $\bar{\nu}_r$, ν'_r, $\bar{\nu}_s$, and ν'_s are proportionality constants which relate the magnitude of the stiffener loading to the plate loading. The substitution of Eqs. (55) through (58) into Eqs. (30) and (31) gives the expressions for the equivalent in-plane edge loads N_x^* and N_y^* for the orthotropic plate, which are

$$N_x^*(t)=N_{xo}^*+N_{xt}^*\cos\theta t \qquad \text{--- (59)}$$

and

$$N_y^*(t) = N_{yo}^* + N_{yt}^* \cos\theta t \qquad \text{--- (60)}$$

in which

$$N_{xo}^* = N_{xo}\left(1 + \frac{A_r \bar{V}_r}{dh}\right) \qquad \text{--- (61)}$$

$$N_{xt}^* = N_{xt}\left(1 + \frac{A_r V_r'}{dh}\right) \qquad \text{--- (62)}$$

$$N_{yo}^* = \bar{\mu} N_{xo}\left(1 + \frac{A_s \bar{V}_s}{\ell h}\right) \qquad \text{--- (63)}$$

and

$$N_{yt}^* = \mu' N_{xt}\left(1 + \frac{A_s V_s'}{\ell h}\right) \qquad \text{--- (64)}$$

The substitution of Eqs. (59) and (60) into Eq. (54) yields

$$\left(M + \frac{n^2\pi^2}{b^2}M' + \frac{m^2\pi^2}{a^2}M''\right)\ddot{T}_{mn} + \left[\left(\frac{m^4\pi^4}{a^4}D_x + \frac{2n^2m^2\pi^4}{a^2b^2}H + \right.\right.$$

$$\left. + \frac{n^4\pi^4}{b^4}D_y\right) - \left(\frac{m^2\pi^2}{a^2}N_{xo}^* + \frac{n^2\pi^2}{b^2}N_{yo}^*\right) - \left(\frac{m^2\pi^2}{a^2}N_{xt}^* + \right.$$

$$\left.\left. + \frac{n^2\pi^2}{b^2}N_{yt}^*\right)\cos\theta t\right]T_{mn} = 0 \qquad \text{--- (65)}$$

for $m = 1, 2, --\infty$, $n - 1, 2, --\infty$. Equation (65) can also be written in the following form

$$A_{mn}\ddot{T}_{mn}(t) + \left[B_{mn} - N_{xo}\left(C_m + \bar{\mu}D_n\right) - N_{xt}\left(\bar{C}_m + \mu D_n\right)\cdot\right.$$

$$\left.\cdot\cos\theta t\right]T_{mn} = 0 \quad , m, n = 1, 2, 3, -----, \infty \qquad \text{--- (66)}$$

in which

$$A_{mn} = \left(M \quad \frac{n^2\pi^2}{b^2} M' + \frac{m^2\pi^2}{a^2} M'' \right) \qquad \text{--- (67)}$$

$$B_{mn} = \left(\frac{m^4\pi^4}{a^4} D_x + \frac{2n^2m^2\pi^4}{a^2b^2} H + \frac{n^4\pi^4}{b^4} D_y \right) \qquad \text{--- (68)}$$

$$C_m = \frac{m^2\pi^2}{a^2} \left(1 + \frac{A_r \overline{V}_r}{dh} \right) \qquad \text{--- (69)}$$

$$\overline{C}_m = \frac{m^2\pi^2}{a^2} \left(1 + \frac{A_r V_r'}{dh} \right) \qquad \text{--- (70)}$$

$$D_n = \frac{n^2\pi^2}{b^2} \left(1 + \frac{A_s \overline{V}_s}{\ell h} \right) \qquad \text{--- (71)}$$

and

$$\overline{D}_n = \frac{n^2\pi^2}{b^2} \left(1 + \frac{A_s V_s'}{\ell h} \right) \qquad \text{--- (72)}$$

The division of Eq. (66) by $[B_{mn} - N_{xo} \; (C_m + \bar{\mu} D_n)]$ and the subsequent rearrangement of the resulting expression yields

$$\ddot{T}_{mn}(t) + \Omega^2_{mn} (1 - 2\mu_{mn} \cos\theta t) T_{mn}(t) = 0 \, , \; m, n = 1, 2, \text{-----}, \infty \qquad \text{--- (73)}$$

in which

$$\Omega^2_{mn} = \frac{B_{mn} - N_{xo} (C_m + \bar{\mu} D_n)}{A_{mn}} \qquad \text{--- (74)}$$

and

$$\mu_{mn} = \frac{N_{xt} (\overline{C}_m + \mu' \overline{D}_n)}{2[B_{mn} - N_{xo} (C_m + \bar{\mu} D_n)]} \qquad \text{--- (75)}$$

Later on it is shown that the expression for the static buckling load, N_{xcr}, has the form

$$N_{xcr} = \frac{B_{mn}}{(C_m + \bar{\mu} D_n)} \qquad \text{--- (76)}$$

The substitution of Eq. (76) into Eq. (65) gives

$$\mu_{mn} = \frac{N_x t \; (\bar{C}_m + \mu' \bar{D}_n)}{2\,[(C_m + \bar{\mu}\, D_n)(N_{xcr} - N_{xo})]} \quad \text{--- (77)}$$

When $\bar{\nu}_r = \nu'_r = \bar{\nu}_s = \nu'_s = 1$, which represents the same magnitude of stress on both the plate and stiffeners, Eq. (77) reduces to

$$\mu_{mn} = \frac{N_x t}{2\,(N_{xcr} - N_{xo})} \quad \text{--- (78)}$$

It is also shown in the next section that Ω_{mn} as given in Eq. (74) is the natural frequency for the equivalent orthotropic plate.

Since the form of Eq. (73) is identical for all m and n the indices can be omitted, hence

$$\ddot{T}(t) + \Omega^2\,(1 - 2\mu \cos\theta t)\;\; T(t) = 0 \quad \text{--- (79)}$$

This equation is the well known Mathieu's equation

2.6 Solution of the Differential Equation with Periodic Coefficients

Equation (79) can be reduced from a second order equation to a system of two first order equations. For this purpose, Eq. (79) is expressed in the form

$$\ddot{T}(t) + B(t)\;\; T(t) = 0 \quad \text{--- (80)}$$

in which

$$B(t) = \Omega^2\,(1 - \mu \cos\theta t) \quad \text{--- (81)}$$

The introduction of the new variables

$$X_1(t) = T(t) \quad \text{--- (82)}$$

and

$$X_2(t) = \dot{T}(t) \quad \text{--- (83)}$$

into Eq. (80) reduces it to the following two differential equations

$$\dot{X}_1(t) - X_2(t) = 0 \quad \text{--- (84)}$$

and

$$\dot{X}_2(t) + B(t)\,X_1(t) = 0 \quad \text{--- (85)}$$

Equations (84) and (85) can be combined through the use of matrix notation to give

$$\{\dot{X}\} + [B(t)]\{X\} = \{0\} \quad \text{--- (86)}$$

in which $\{x\}$ is a column matrix (vector) with components $x_1(t)$ and $x_2(t)$ and

$$[B(t)] = \begin{bmatrix} 0 & -1 \\ B(t) & 0 \end{bmatrix} \quad \text{--- (87)}$$

a square matrix of the second order.

The theory associated with the solution of Eq. (86) is discussed in references (39, 46). The results of the theory reveal that the solution of Eq. (79) or (86) is bounded (stable response) over certain defined regions and is unbounded (unstable response) over the remaining defined regions. The boundaries between the stable and unstable response regions are characterized by the periodic solutions

$$T(t+T') = T(t) \quad \text{--- (88)}$$

with period T' and

$$T(t+T') = -T(t) \quad \text{--- (89)}$$

with period 2T'. Since this investigation is concerned with the onset of parametric resonance it is thus necessary to determine the conditions for which Eq. (79) or (86) has periodic solutions. Since the required solutions are periodic, they can be expressed in terms of a Fourier series, thus for a region of 2T'

$$T_1(t) = \frac{a_o}{2} + \sum_{K=1}^{\infty}\left[a_K \cos\frac{K\theta t}{2} + b_K \sin\frac{K\theta t}{2}\right] \quad \text{--- (90)}$$

represents the solutions with period T' and

$$T_2(t) = \frac{c_o}{2} + \sum_{K=1}^{\infty}\left[c_K \cos\frac{K\theta t}{2} + d_K \sin\frac{K\theta t}{2}\right] \quad \text{--- (91)}$$

represents the solutions with period 2T'. Here the period T' is given by $2\pi/\theta$. These series converge since the periodic solutions satisfy the Dirichlet conditions. The coefficients a_k and b_k can be evaluated through the use of the expressions

$$a_o = \frac{1}{T'}\int_0^{2T'} T(t)\, dt \quad \text{--- (92)}$$

$$a_K = \frac{1}{T'}\int_0^{2T'} T(t) \cos\frac{K\theta t}{2}\, dt \quad \text{--- (93)}$$

$$b_K = \frac{1}{T''}\int_0^{2T'} T(t) \sin\frac{K\theta t}{2}\, dt \quad \text{--- (94)}$$

and Eq. (88). The evaluation of the coefficients yields the following information

$$a_o = \frac{2}{T'}\int_0^{T'} T(t)\, dt \quad \text{--- (95)}$$

$$a_K = \left\{\begin{array}{ll} \frac{2}{T'}\int_0^{T'} T(t) \cos\frac{K\pi t}{T'}\, dt & , K = 2, 4, 6, ---- \\ 0 & , K = 1, 3, 5, ---- \end{array}\right\} \quad \text{--- (96)}$$

$$b_K = \begin{cases} \dfrac{2}{T'}\displaystyle\int_0^{T'} T(t)\sin\dfrac{K\pi t}{T'} & , K = 2, 4, 6, \text{----} \\ 0 & ; K = 1, 3, 5, \text{----} \end{cases} \quad \text{---} \ (97)$$

The application of the information contained in Eqs. (95) through (97) to Eq. (90) reduces it to the form

$$T_1(t) = \frac{a_0}{2} + \sum_{K=2,4,\cdots}^{\infty}\left[a_K \cos\frac{K\theta t}{2} + b_K \sin\frac{K\theta t}{2}\right] \quad \text{---} \ (98)$$

In a similar manner, Eq. (91) can be reduced to

$$T_2(t) = \sum_{K=1,3,\cdots}^{\infty}\left[c_K \cos\frac{K\theta t}{2} + d_K \sin\frac{K\theta t}{2}\right] \quad \text{---} \ (99)$$

The substitution of Eq. (98) into Eq. (79) and combining like terms of 1, cos $\frac{k\theta t}{2}$ and sin $\frac{k\theta t}{2}$ and dividing by Ω^2 yields

$$\frac{a_0}{2} - a_0\mu\cos\theta t + \sum_{K=2,4}^{\infty}\left\{\left[\frac{-K^2\theta^2}{4\Omega^2} + 1\right]a_K\cos\frac{K\theta t}{2} + \right.$$

$$+\left[\frac{-K^2\theta}{4\Omega^2} + 1\right]b_K\sin\frac{K\theta t}{2} - a_K 2\mu\cos\theta t\cos\frac{K\theta t}{2} -$$

$$\left. -b_K 2\mu\cos\theta t\sin\frac{K\theta t}{2}\right\} = 0 \quad \text{---} \ (100)$$

However

$$a_K\cos\theta t\cos\frac{K\theta t}{2} = \begin{cases} \dfrac{a_2}{2} & , K = 0 \\ \dfrac{a_4}{2}\cos\theta t & , K = 2 \\ \dfrac{1}{2}\cos\dfrac{K\theta t}{2}\left(a_{(K+2)} + a_{(K-2)}\right) & , K\ 4, 6, \text{--} \end{cases} \quad \text{---} \ (101)$$

and

$$b_K \cos\theta t \sin\frac{K\theta t}{2} = \begin{cases} \dfrac{b_4}{2}\sin\theta t & ,K=2 \\[2ex] \dfrac{1}{2}\sin\dfrac{K\theta t}{2}\left(b_{(K+2)}+b_{(K-2)}\right) & ,K=4,6,--- \end{cases} \qquad --- (102)$$

The substitution of Eqs. (101) and (102) in Eq. (100) gives

$$\frac{a_0}{2} - a_2\mu + \sum_{K=2,4}^{\infty}\left\{\left[-a_{(K-2)}\mu + \left(\frac{-K^2\theta^2}{4\Omega^2}+1\right)a_K - a_{(K+2)}\mu\right]\cos\frac{K\theta t}{2} + \left[-b_{(K-2)}\mu + \left(-\frac{K^2\theta^2}{4\Omega^2}+1\right)b_K - b_{(K+2)}\mu\right]\sin\frac{K\theta t}{2}\right\} = 0 \qquad --- (103)$$

If φ_i is a linearly independent set of functions, then the condition

$$\sum_{i=1}^{\infty} r_i\varphi_i = 0 \qquad --- (104)$$

requires that the r_i's be equal to zero. Equation (103) has the same form as Eq. (104) and the functions 1, $\cos\frac{k\,\theta\,t}{2}$ and $\sin\frac{k\,\theta\,t}{2}$ form a linearly independent set of functions. Thus, the coefficients of Eq. (103) are equal to zero, which implies that

$$\frac{a_0}{2} - a_2\mu = 0 \qquad --- (105)$$

$$-a_{(K-2)}\mu + \left(\frac{-K^2\theta^2}{4\Omega^2}+1\right) a_K - a_{(K+2)}\mu = 0, K=2,4,6,--- \quad (106)$$

$$\left(\frac{-\theta^2}{\Omega^2}+1\right) b_2 - b_4\mu = 0 \quad --- \quad (107)$$

and

$$-b_{(K-2)}\mu + \left(\frac{-K^2\theta^2}{4\Omega^2}+1\right) b_K - b_{(K+2)}\mu = 0 \quad , K=2,4,6,--- \quad (108)$$

The multiplication of Eq. (105) by 2, Eq. (106) by 1/4 for k = 2 and Eq. (106) by $1/k^2$ for k = 4,6,--- yields

$$a_0 = 2\mu a_2 \quad --- \quad (109)$$

$$-\frac{\mu}{4} a_0 + \left(\frac{1}{4}-\delta\right) a_2 - \frac{\mu}{4} a_4 = 0 \quad --- \quad (110)$$

and

$$-\frac{\mu}{K^2} a_{(K-2)} + \left(\frac{1}{K^2}-\delta\right) a_K - \frac{\mu}{K^2} a_{(K+2)} = 0 \quad ,K=4,6,---- \quad --- \quad (111)$$

in which

$$\delta = \frac{\theta^2}{4\Omega^2} \quad --- \quad (112)$$

The substitution of Eq. (109) into Eq. (110) gives

$$\left[\left(-\frac{\mu^2}{2}+\frac{1}{4}\right)-\delta\right]a_2-\frac{\mu}{4}a_4=0 \qquad \text{--- (113)}$$

The introduction of the parameter δ into Eqs. (107) and (108) yields

$$\left(\frac{1}{4}-\delta\right)b_2-\frac{\mu}{4}b_4=0 \qquad \text{--- (114)}$$

$$-\frac{\mu}{K^2}b_{(K-2)}+\left(\frac{1}{K^2}-\delta\right)b_K-\frac{\mu}{K^2}b_{(K+2)}=0,\ K=4,6,--- \qquad (115)$$

The first system of equations, Eqs. (111) and (113) contains only a_k coefficients and the second system of equations, Eqs. (114) and (115) contains only b_k coefficients. The existence of non-trivial solutions for the above two systems of homogeneous equations requires that the a_k and b_k coefficients be non-zero. This condition requires that the determinant of the coefficients of each of the two systems be equal to zero. Hence, the condition for the existence of periodic solutions with period $2\pi/\omega$ has the form

$$\det.\left([A]_1-\delta\,[I]\right)=0 \qquad \text{--- (116)}$$

and

$$\det.\left([A]_2-\delta\,[I]\right)=0 \qquad \text{--- (117)}$$

in which $[I]$ is the unit matrix,

$$[A]_1 = \begin{bmatrix} \left(-\frac{\mu^2}{2}+\frac{1}{4}\right) & -\frac{\mu}{4} & 0 \\ -\frac{\mu}{16} & \frac{1}{16} & -\frac{\mu}{16} \\ 0 & -\frac{\mu}{36} & \frac{1}{36} \end{bmatrix} \qquad \text{--- (118)}$$

and

$$A_2 = \begin{bmatrix} \frac{1}{4} & -\frac{\mu}{4} & 0 \\ -\frac{\mu}{16} & \frac{1}{16} & -\frac{\mu}{16} \\ 0 & -\frac{\mu}{36} & \frac{1}{36} \end{bmatrix} \qquad \text{--- (119)}$$

The parameters $\Omega 2, \mu$, and δ are given by Eqs. (74), (75) and (112) respectively. Similarily the substitution of Eq. (99) into Eq. (79) yields the conditions for the existence of periodic solutions with a period $4\pi/\theta$, which are

$$\det.\left([A]_3 - \delta [I]\right) = 0 \qquad \text{--- (120)}$$

and

$$\det.\left([A]_4 - \delta [I]\right) = 0 \qquad \text{--- (121)}$$

in which

$$[A]_3 = \begin{bmatrix} 1-\mu & -\mu & 0 \\ -\frac{\mu}{9} & \frac{1}{9} & -\frac{\mu}{9} \\ 0 & -\frac{\mu}{25} & \frac{1}{25} \end{bmatrix} \qquad \text{--- (122)}$$

and

$$[A]_4 = \begin{bmatrix} 1+\mu & -\mu & 0 \\ -\frac{\mu}{9} & \frac{1}{9} & -\frac{\mu}{9} \\ 0 & -\frac{\mu}{25} & \frac{1}{25} \end{bmatrix} \qquad \text{--- (123)}$$

The eigenvalues, γ, which are necessary for the existence of periodic solutions of Eq. (66) are determined numerically from Eqs. (116), (117), (120) and (121).

Finally it can be shown that for $\mu \to 0$ there exist periodic solutions with period 2T in the vicinity of

$$\theta = \frac{2\Omega}{K}, K = 1, 3, 5, \text{------} \qquad \text{--- (124)}$$

and periodic solutions with period T in the vicinity of

$$\theta = \frac{2\Omega}{K}, K = 2, 4, 6, \text{------} \qquad \text{--- (125)}$$

Equations (124) and (125) give a relationship between the frequency of the in-plane boundary forces and the frequencies of the free vibrations of the stiffened plate, near which the formation of unboundedly increasing vibrations is possible. Thus, these relationships define the vicinity of the regions of parametric instability for a stiffened plate. Also, Eqs. (124) and (125) indicate that there exists an infinite number of regions associated with each Ω. Somerset (20) calls the mode associated with a particular value of Ω as the spatial mode and each mode associated with Eqs. (124) and (125) for a given spatial mode is called a temporal mode. This nomenclature is adopted in this investigation.

2.7 Special Cases

a. Natural Vibration Case

This section is concerned with the determination of the natural frequencies for the equivalent orthotropic plate subjected to static in-plane edge forces. When the variable components N_{xt} and N_{yt} of the harmonic in-plane loading are equal to zero, Eq. (79) reduces to the form

$$\ddot{T}(t) + \Omega^2 T(t) = 0 \qquad \text{--- (126)}$$

If a solution to Eq. (126) is sought in the form

$$T t = \exp\left[\lambda t\right] \qquad \text{--- (127)}$$

Then the substitution of Eq. (127) into Eq. (126) yields

$$\lambda = \pm i\,\Omega \qquad \text{--- (128)}$$

Thus the solution of Eq. (124) is

$$T(t) = A_1 \exp\left[i\Omega t\right] + B_1 \exp\left[-i\Omega t\right] \qquad \text{--- (129)}$$

or

$$T(t) = C_1 \cos \Omega t + D_1 \sin \Omega t \qquad \text{--- (130)}$$

in which

$$C_1 = A_1 + B_1 \qquad \text{--- (131)}$$

and

$$D_1 = i\,(A_1 - B_1) \qquad \text{--- (132)}$$

From Eq. (130) it is seen that Ω given by Eq. (74) represents the natural frequencies of the equivalent orthotropic plate for a specific value of N_{xo} and Π.

When the effect of rotatory inertia is neglected and when N_{xo} and N_{yo} are equal to zero, Eq. (74) reduces to the form

$$\Omega^2_{mn} = \frac{B_{mn}}{A_{mn}} \qquad \text{--- (133)}$$

in which

$$A_{mn} = M \qquad \text{--- (134)}$$

Equation (133) can be written in an expanded form in terms of the elastic and geometric properties of a stiffened plate with uniform material properties, which is

$$\Omega^2_{mn} = \left\{m^4\left(1+\frac{n^2\beta^2}{m^2}\right)^2 + m^4\left[\frac{E_r I_r}{Dd} + \frac{n^2\beta^2}{m^2}\left(\frac{G_r J_r}{Dd} + \frac{G_s J_s}{D\ell}\right) + \frac{n^4\beta^4}{m^4}\,\frac{E_s I_s}{D\ell}\right]\right\} \Big/ \frac{M a^4}{\pi^4 D} \qquad \text{--- (135)}$$

in which $\beta = a/b$. This equation agrees with the results obtained by Mikulas and McElman (37) for the same case. If Eq. (74), for the case of N_{xo} and N_{yo} equal to zero, is written in an expanded form in terms of the orthotropic rigidity constants, then it gives

$$\Omega^2_{mn} = \pi^4\left[\frac{m^4}{a^4}D_x + 2\frac{n^2 m^2}{a^2 b^2}H + \frac{n^4}{b^4}D_y\right] \Big/ \left[M + \pi^2\left(\frac{n^2}{b^2}M' + \frac{m^2}{a^2}M''\right)\right] \qquad \text{--- (136)}$$

This equation agrees with the results obtained by Hoppman (47).

b. Static Stability Case

This section is concerned with the case of static stability of the equivalent orthotropic plate. This case corresponds to the conditions that N_{xo} is not specified and that N_{xt} is equal to zero. Also for this case the deflection of the orthotropic plate is independent of time. Subject to these conditions Eq. (73) takes the form

$$\left[B_{mn} - N_{xo}\left(C_m + \mu D_n\right)\right] T_{mn} = 0, \quad m,n = 1,2,\text{-----}\infty \qquad \text{--- (137)}$$

in which T_{mn} is a constant. The condition for the existence of a non-trivial solution of Eq. (137) yields

$$(N_{xo})_{cr} = \frac{B_{mn}}{(C_m + \Omega D_n)} \qquad \text{--- (138)}$$

in which N_{xcr} is the critical buckling load. For a plate with only in-plane loading in the x-direction, that is = 0, Eq. (138) reduces to

$$(N_{xo})_{cr} = \frac{B_{mn}}{C_m} \qquad \text{--- (139)}$$

Equation (139) can be written in the following expanded form

$$(N_{xo})_{cr} = \left[\frac{m^4 \pi^4}{a^4} D_x + 2\frac{m^2 n^2 \pi^4}{a^2 b^2} H + \frac{n^4 \pi^4}{b^4_y} D_y\right] \Big/ \frac{m^2 \pi^2}{a^2} \cdot$$

$$\cdot \left(1 + \frac{A_r \overline{\nabla}_r}{dh}\right) \qquad \text{--- (140)}$$

When m = n = 1 the equivalent orthotropic plate buckles into a one-half sine wave mode. For this case when $\overline{\nabla}_r = 1$, Eq. (140) takes the form

$$(N_{xo})_{cr} = \frac{\pi^2}{b^2}\left[\frac{b^2}{a^2} D_x + 2H + \frac{a^2}{b^2} D_y\right] \Big/ \left(\frac{A_r}{t} + 1\right) \qquad \text{--- (141)}$$

This equation agrees with the result given by Timoskenko and Gere (48).

3. RESULTS

The theory developed in Section 2 led to the determination of the eigenvalues of four matrices for the problem studied. The numerical procedure used to determine the eigenvalues of these matrices is based on the idea of reducing the original matrix to a similar matrix whose eigenvalues are much easier to determine.

The algorithm used in this investigation to reduce the matrices to similar matrices was developed by Francis (49, 50, 51) which he calls QR-Transformation. The computer subroutines based on this algorithm are from the SHARE library program package 3006-01 and were written by Imad and VanNess (52).

3.1 Convergence Studies

The theory developed in Section 2 for the orthotropic plate resulted in separate but similar differential equations for the determination of the unknown time functions which are the coefficients of a series which represents the deflection function w(x,y,t) of the stiffened plate. Each of these differential equations had the form of Mathieu's equation. The solution for each of these differential equations was represented by a Fourier series and this led to the determination of the eigenvalues of four matrices whose size was dependent on the number of terms taken in the Fourier series. The square root of the eigenvalues of these four matrices represents the value of $\Theta/2\Omega$ on the boundaries of the regions of instability. Figure 12, which is valid for any spatial mode, shows the first eight temporal mode regions. In section 2.6 it was shown that a temporal mode existed for each term of the Fourier series.

The convergence curves given by Figs. 4 through 11 shows how many terms of the Fourier series are needed to obtain what appears to be convergence of the magnitude of the eigenvalues for a specific example. These eight graphs represent the value of $\Theta/2\Omega$ on the upper and lower boundaries of the first four temporal modes at $\mu = 1.2$, where μ is the abscissa of Fig. 12. A study of the convergence characteristics of the magnitude of the square root of the eigenvalues showed that more terms were needed to obtain convergence as the value of μ was increased and as the order of the highest temporal mode was increased. Thus $\mu = 1.2$ represents an extreme case. Examination of the eight convergence curves shows that the value $\Theta/2\Omega$ for the lower curve of the fourth temporal mode is the slowest to converge but it does appear to have converged to the correct value for an eight term approximation. The value of $\Theta/2\Omega$ for the eighth and tenth term approximation is the same for the first six significant figures. However, the error between the sixth and tenth term approximation is less than one tenth of one percent. The error in the magnitude of the eigenvalues must be kept small in order to prevent misleading over-lapping of the temporal modes, expecially the higher order temporal modes.

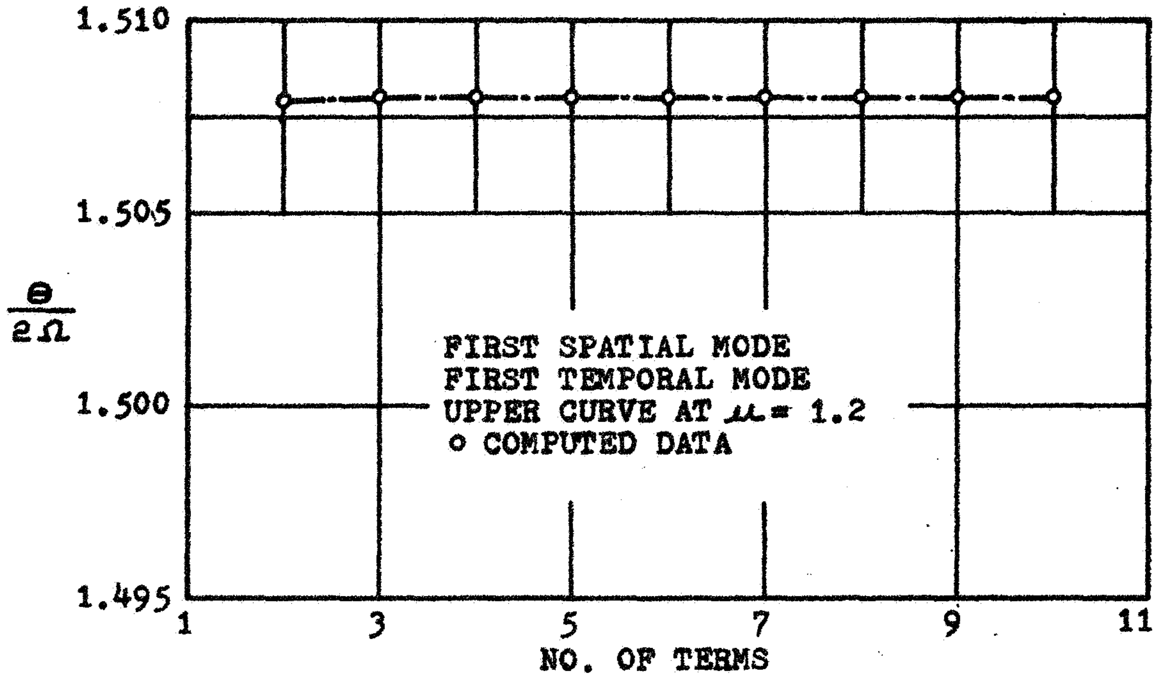

Fig. 4 Convergence Curve Associated with Mathieu's Equation First Temporal Mode Upper Curve

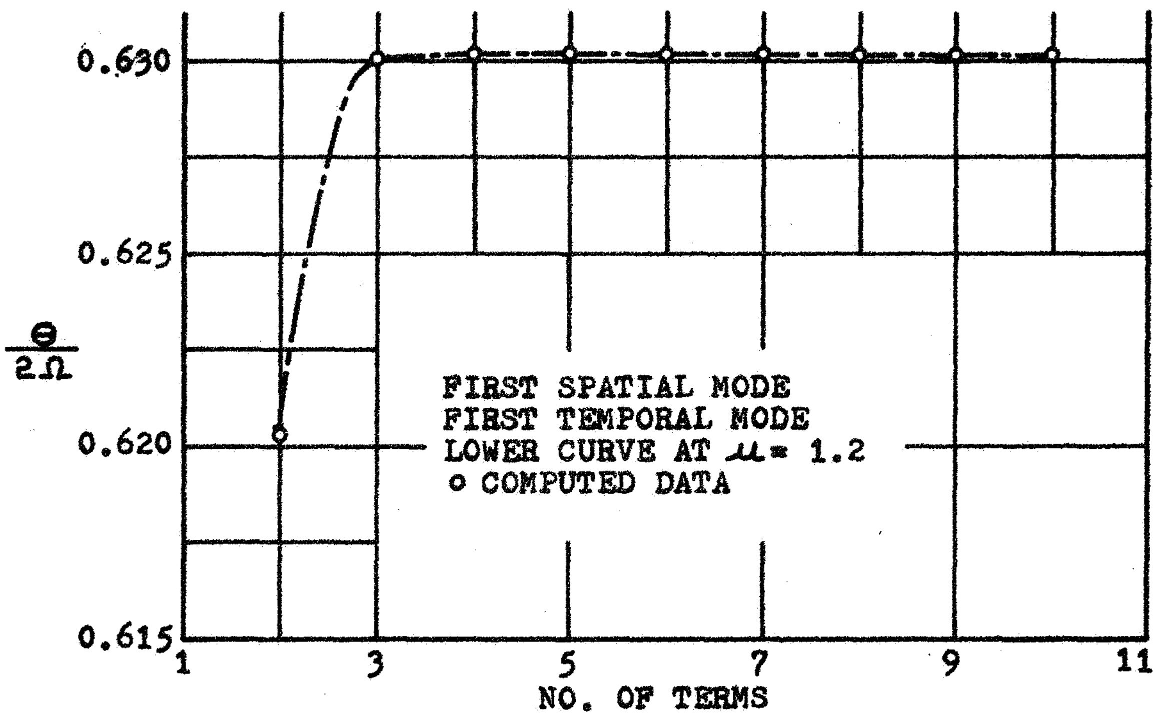

Fig. 5 Convergence Curve Associated with Mathieu's Equation First temporal Mode Lower Curve

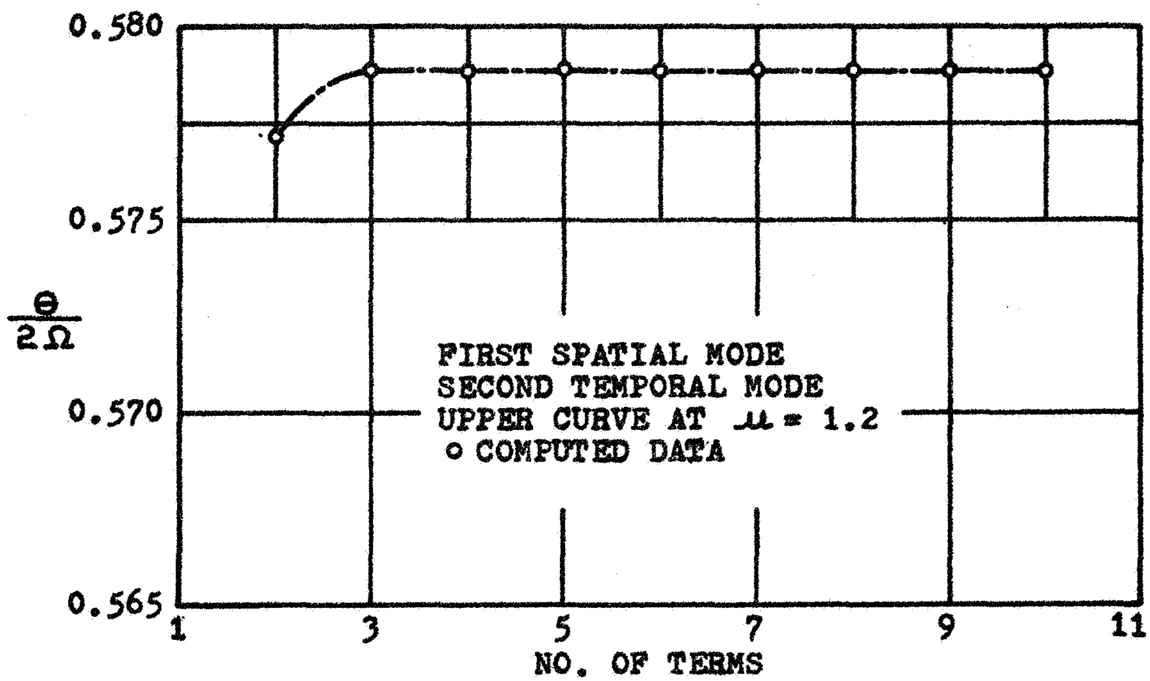

Fig. 6 Convergence Curve Associated with Mathieu's Equation Second Temporal Mode Upper Curve

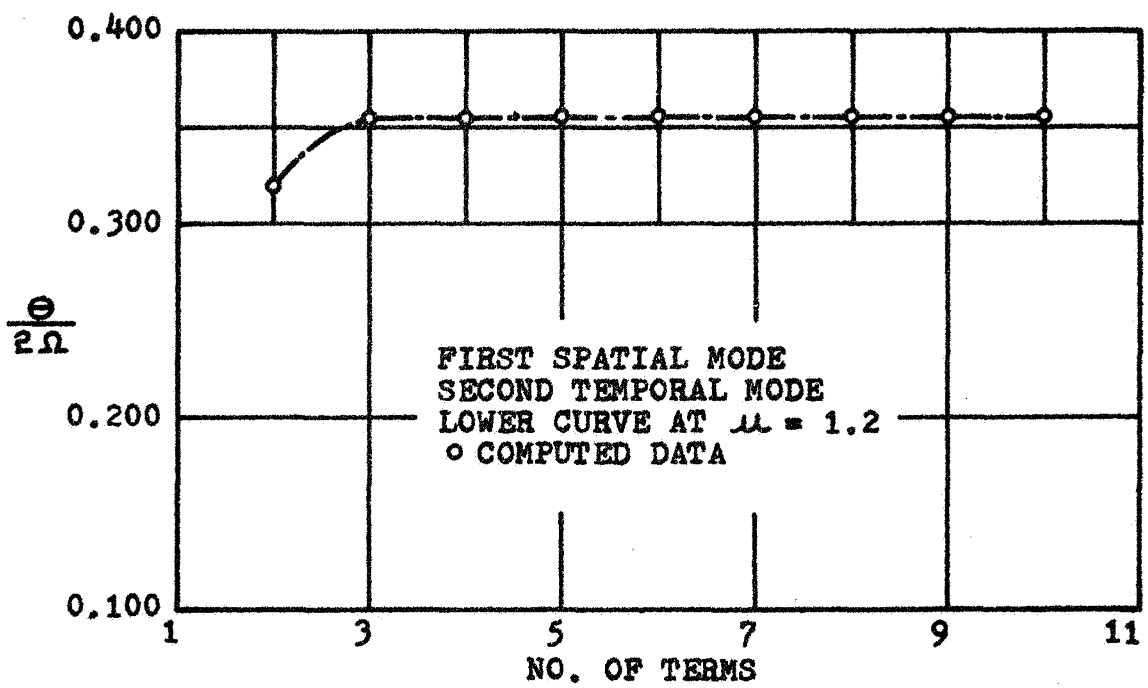

Fig. 7 Convergence Curve Associated with Mathieu's Equations Second Temporal Mode Lower Curve

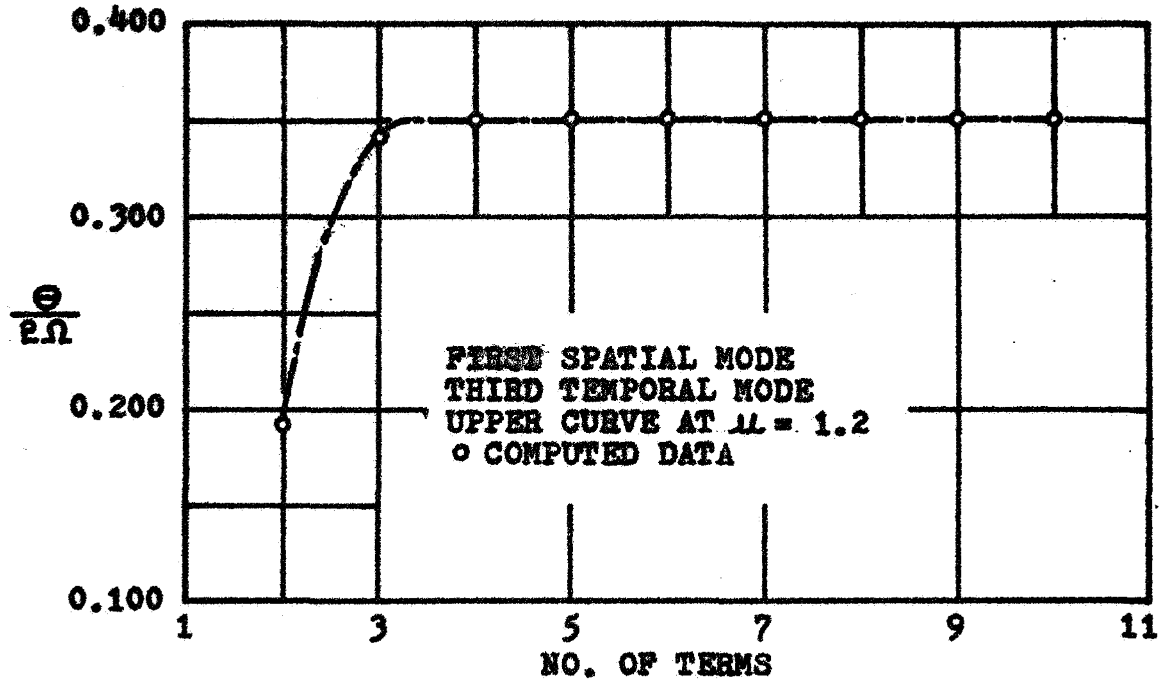

Fig. 8 Convergence Curve Associated with Mathieu's Equation Third Temporal Mode Upper Curve

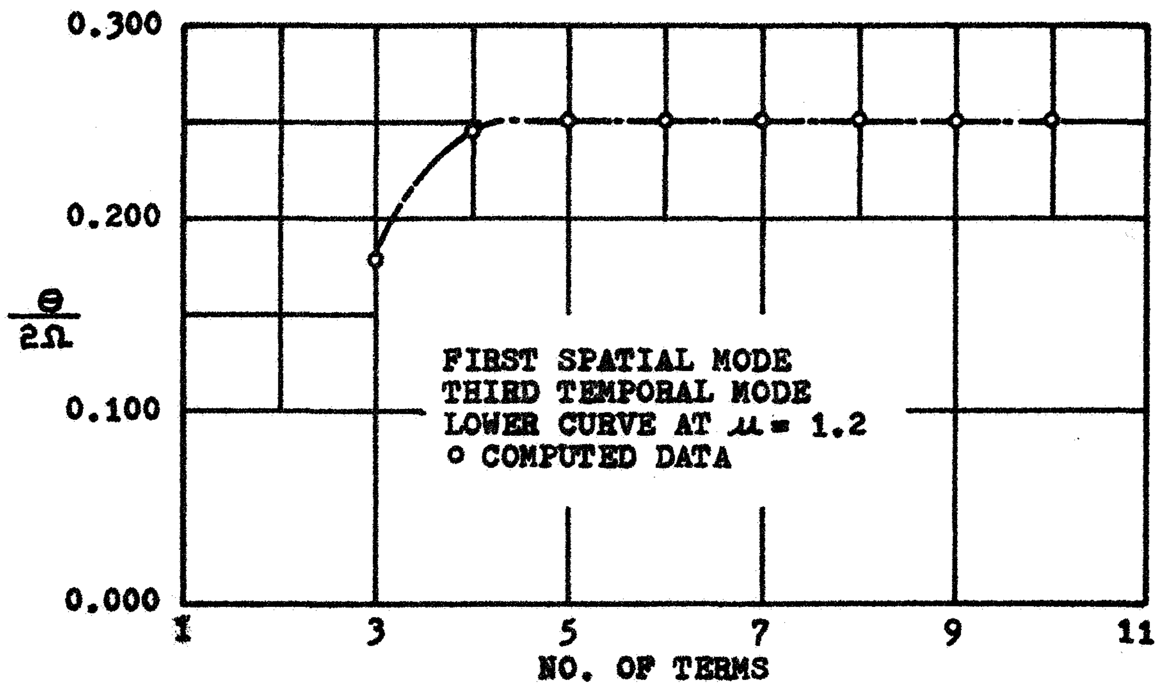

Fig. 9 Convergence Curve Associated with Mathieu's Equation 3rd Temporal Mode Lower Curve

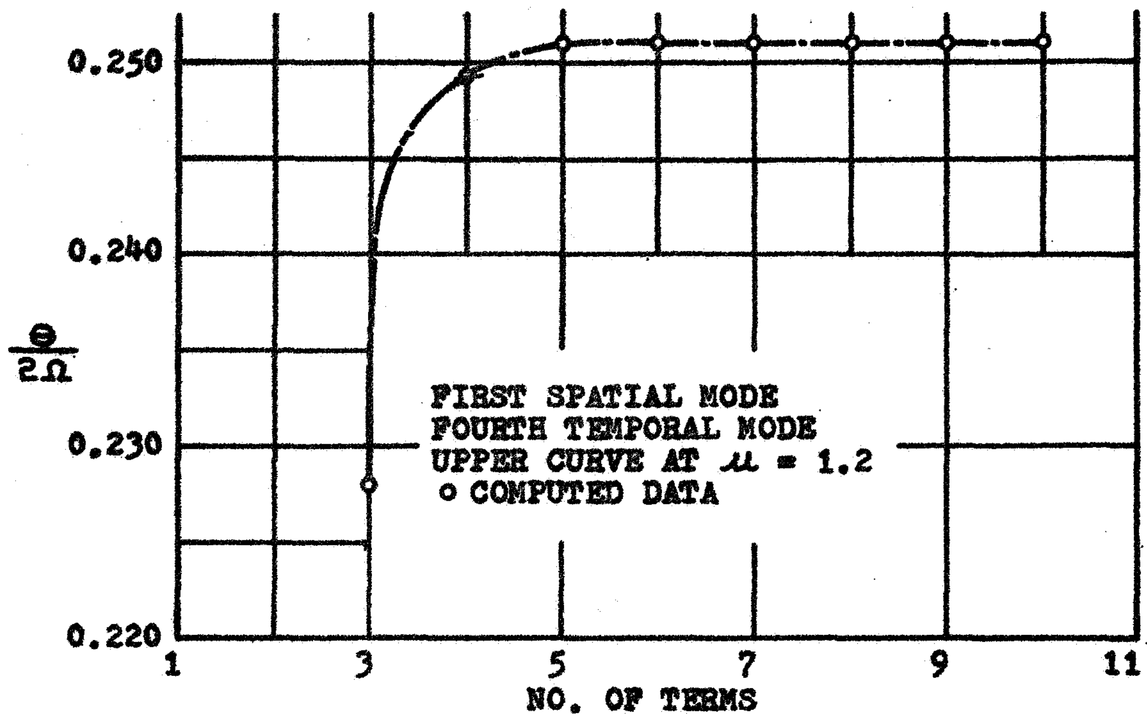

Fig. 10 Convergence Curve Associated with Mathieu's Equation Fourth Temporal Mode Upper Curve

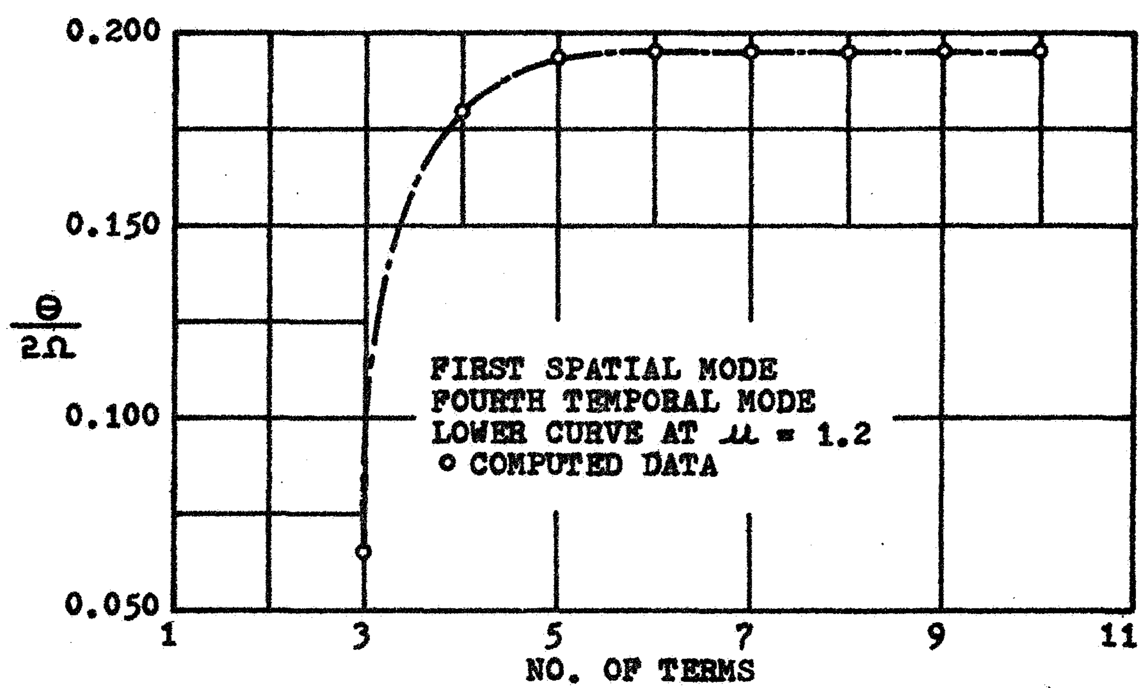

Fig. 11 Convergence Curve Associated with Mathieu's Equation Fourth Temporal Mode Lower Curve

3.2 Theoretical Results

The results for the parametric response of an orthotropic plate are given by Fig. 12. These results plotted in the $(\mu, \Theta/2\Omega)$ parameter space represent the eigenvalues, $\Theta/2\Omega$, obtained from the matrices $[B]_1$, through $[B]_4$ associated with the solution of Mathieu's function. The square root of the eigenvalues correspond to the values of $\Theta/2\Omega$ on the boundaries between the regions of stability and instability. These results are also presented in table form in Tables One through Three in the Appendix. If a given value of Θ and the values of Ω and μ calculated from Eqs. (74) and (75) respectively for a given stiffened plate, are such that the parameters μ and $\Theta/2\Omega$ fall within the shaded areas given by Fig. 12, then the stiffened plate is in an unstable condition. Figure 12 shows that the principal region of instability, that is the one associated with $\Theta/2\Omega = 1$, is the most dangerous since it is the widest. The results show that the width of the regions of instability decreases for the higher order temporal mode regions. The results also reveal that, if possible, the orthotropic plate should be designed so that the parameters μ and $\Theta/2\Omega$ fall within the stable regions.

The format of Fig. 12 is slightly different but similar to the Strutt diagram normally associated with Mathieu's equation. The form chosen seems to be more convenient for engineering purposes. The results given by Fig. 12 are the most complete set of results known in terms of the number of instability regions presented and the range over which μ is taken for this particular form of presentation. It took sixteen terms of the Fourier series solution of Mathieu's equation to obtain the results presented. The instability regions obtained from Mathieu's equation which are presented in previously published investigations (1, 25, 44) appear to be based on just a two or three term approximation since the computation of the eigenvalues can be done by hand. A two term approximation of the instability regions up to $\mu = 0.6$ is given by Figure 13. A comparison of Figs. 12 and 13 shows that a two term approximation gives good results for the range of μ presented for the principal region of instability. However, the two term approximation gives increasing poorer results for the higher order regions of instability as μ increases, particularly for the lower stability boundary. Thus a two term approximation leads to incorrect information about the location of the higher order instability regions.

3.3 Evaluation of Results

The theoretical results presented in the last section, Fig. 12, show that the most dangerous region of instability, from the viewpoint of width, is the first temporal mode associated with any spatial mode. This wide width of the

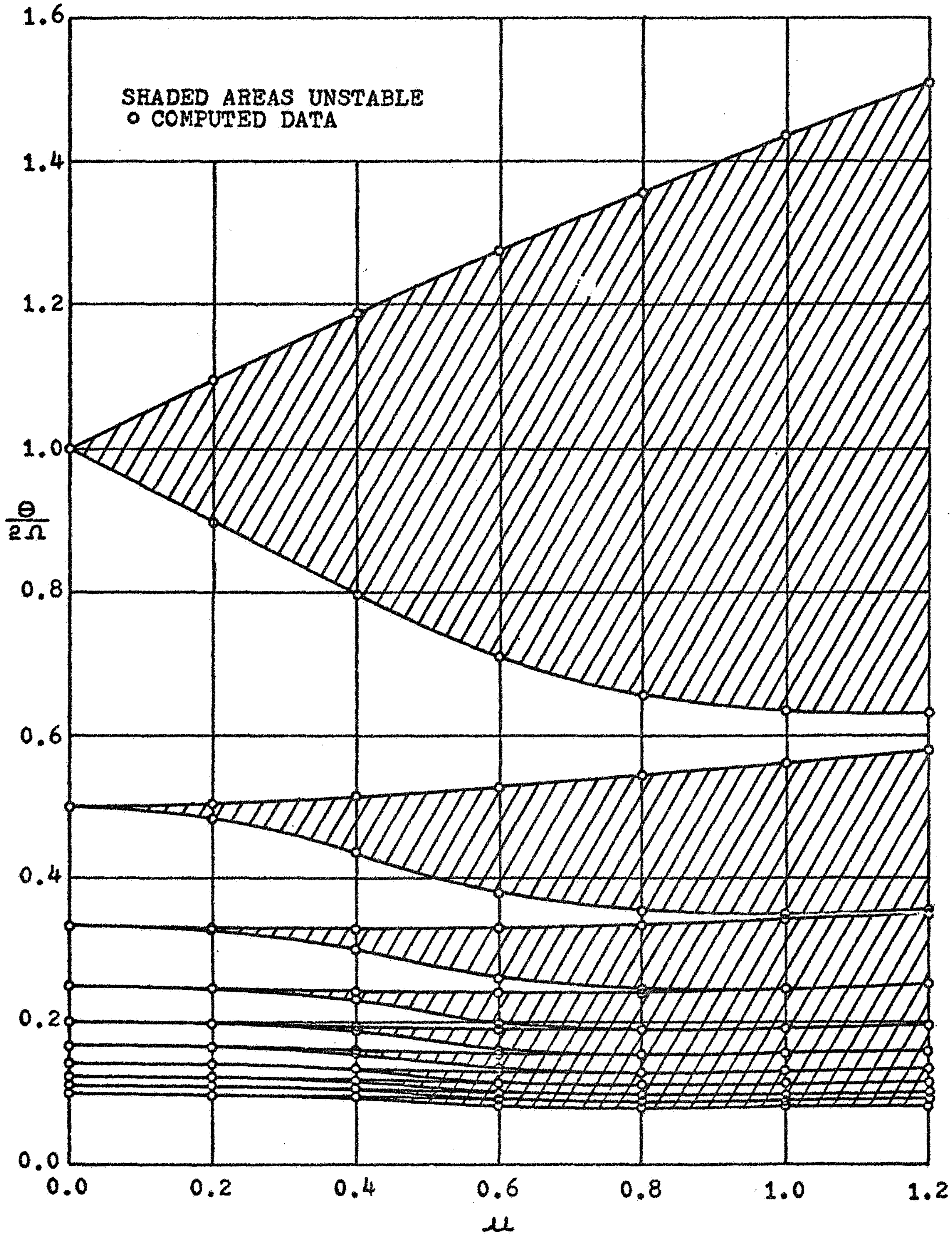

Fig. 12 Parametric Instability Regions Associated with the Orthotropic Model (Mathieu's Equation)

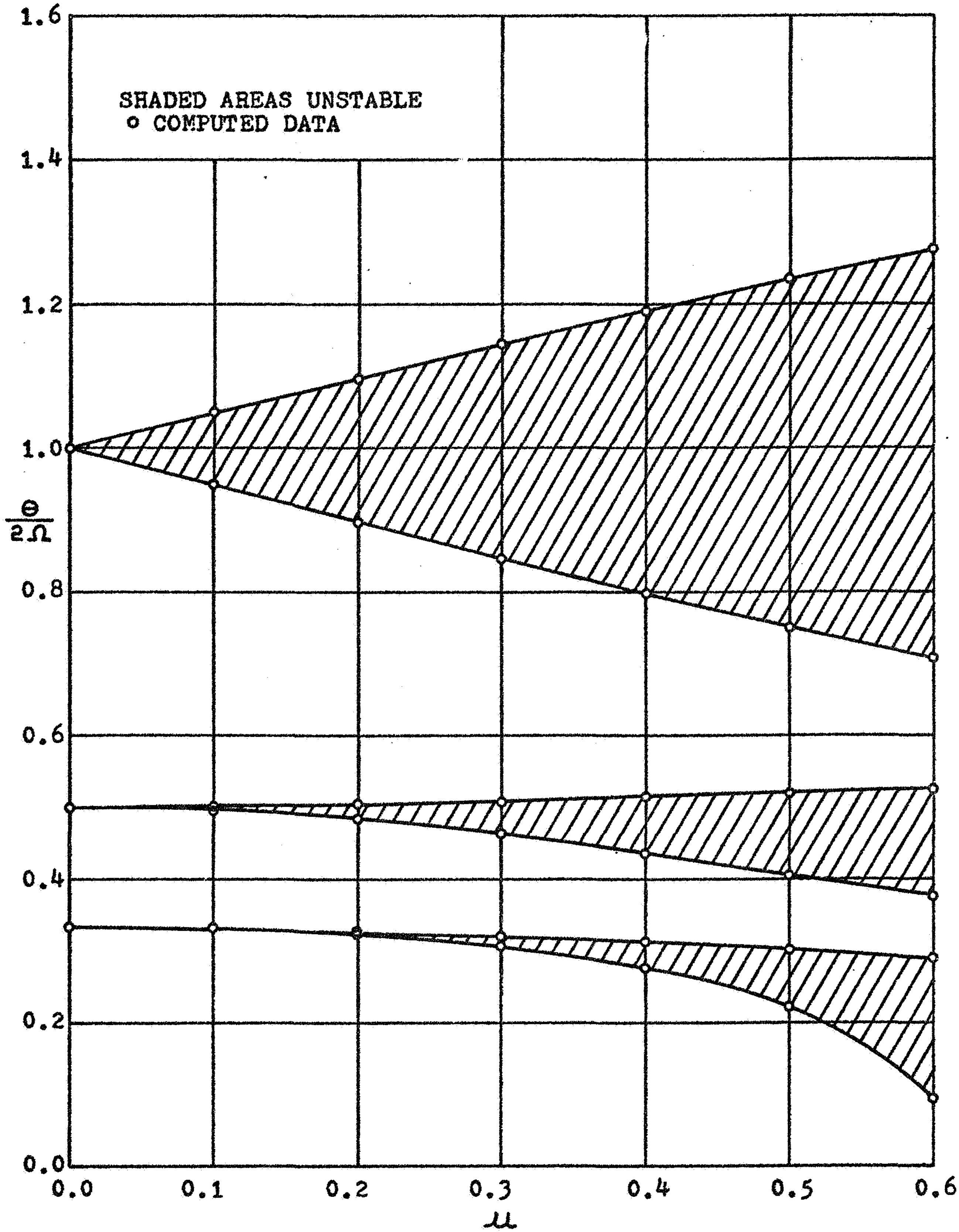

Fig 13. Parametric Instability Regions Associated with the Orthotropic Model for a Two Term Approximation

instability region implies that there is a wide band of frequencies over which the stiffened plate will be unstable. The results also show that widths of the temporal mode regions of instability decrease as the order of the region increases. The narrow width of these higher order regions implies that a small change in the load frequency, Θ , would remove the system from these instability regions. Thus, the higher order regions are not as critical as the lower order regions.

The theory developed in this investigation only predicts the location of the boundaries of the regions of instability. Within these regions of instability the theory gives no information about the behavior of the stiffened plate except that the solution of the problem for these regions is unbounded. This result implies that the transverse amplitude of the plate will grow indefinitely as shown in Fig. 14.

Experimental results obtained from a stiffened plate with a single transverse stiffener (30, 39) also show that the higher the order of the temporal mode region, the less the magnitude of the transverse amplitude. These results appear to indicate that the build-up of the transverse amplitude is not sufficient to cause the higher order temporal modes to be of concern. However, this point does need further investigation. The transverse amplitude of the real stiffened plate reaches an upper limit within a region of instability due to stretching of the middle-surface of the plate.

The results given by Fig. 12 also show that for μ greater than 0.6 and $\Theta/2\Omega$ less than 0.3 the stiffened plate will always be unstable. A stiffened plate passing through the above defined region would go from one temporal mode instability region to another even though the plate is vibrating in an unstable condition. The results indicate that the vibration frequency of the plate would change periodically from a value of Θ to a value of $\Theta/2$, where Θ is the frequency of the in-plane loading. However, the experimental results mentioned above would seem to indicate that this large instability area would not present much of a problem since the transverse amplitude build-up would be very small.

The importance of the first temporal mode and the lesser importance of the higher order temporal modes is further illustrated when damping of the stiffened plate is taken into consideration. The effects of damping on the boundaries of typical instability regions is shown in Fig. 15 which represents the results given by Mathieu's function modified to include damping, see Bolotin (18). Figure 15 shows that damping causes the instability regions to withdraw from the $\Theta/2\Omega$ ordinate. The amount of withdrawal increases as the order of the temporal mode increases. In case of an undamped temporal mode region, the portion of the instability region where the upper and lower

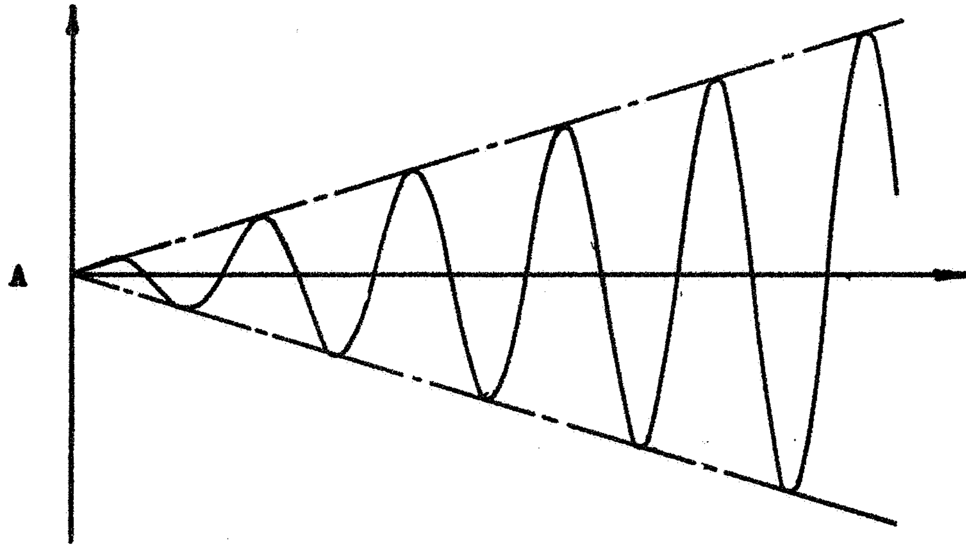

Fig. 14 Build-up of Transverse Amplitude within Instability Region

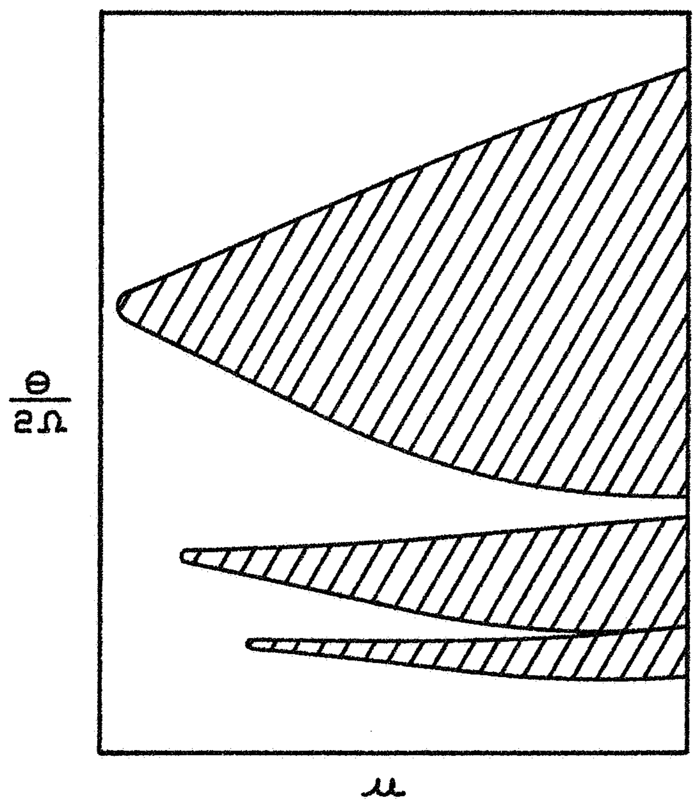

Fig. 15 Typical Instability Regions in the (μ,$\Theta/2\Omega$) Parameter Space (with damping)

boundaries coincide will disappear if a damping is present. Figure 15 thus indicates that the higher order temporal mode instability regions would not exist in a practical range for μ. This result was observed in the experimental investigation conducted on the stiffened plate with a simple transverse stiffener (30, 39). It is also clearly illustrated in Fig. 15 why the principal region of instability is considered to be the most critical as it exists for relatively small values of α'/α_{cr} even when damping is present.

The theoretical results given in section 3.2 are based on a nondimensional representation of the data which is standard practice. However, such representation can lead to misinterpretation of the results. Examination of these results could lead to the mistaken conclusion that the temporal mode instability regions associated with each of the spatial modes are separate from one another. Figure 16 illustrates such an example. This figure is taken from reference (39) and it represents the parametric instability regions for a rectangular plate reinforced with a single transverse stiffener as shown in Figure 17. Figure 16 shows the first two temporal mode regions of instability for each of the first three spatial modes superimposed in the same $(\alpha'/\alpha_{cr}, \sqrt{M}\,\Theta)$ parameter space for a value of $\bar{\alpha}/\alpha_{cr} = 0.5$. The above parameters are defined as follows.

α_{cr} Critical buckling parameter $= b^2N_{xcr}/\pi^2D$

$\bar{\alpha}$ Static in-plane load parameter $= b^2N_{xo}/\pi^2D$

α' Variable in-plane load parameter $= b^2N_{xt}/\pi^2D$

M Mass parameter for the plate $= a^4\rho_p h/4\pi^4D$

As can be seen from Figure 16 the temporal mode regions of instability associated with the various spatial modes can overlap. Figure 16 also shows for large values of $\bar{\alpha}/\alpha_{cr}$ the second temporal mode region of instability associated with the second spatial mode lies partly below the principal region of instability associated with the first spatial mode for values α'/α_{cr} greater than 0.4. Figure 18 illustrates an experimental test run (39) which shows the response of a stiffened plate when temporal mode regions associated with different spatial modes overlap. This figure shows the transient motion of the stiffened plate from the principal region associated with the second spatial mode which overlaps the principal region at this point. Figure 18 also indicates an interaction between the two regions of instability where they overlap. The build-up of amplitude for the second temporal mode region is significant.

The linear theory presented in this investigation does predict the location of the boundaries of the regions of instability at which the onset of parametric response takes place. The knowlege of these boundary locations provides the designer with the necessary information so that a stiffened plate can be designed to operate within the stable regions. In conclusion, when the rectangular plate reinforced with closely spaced stiffeners is analyzed as an equivalent orthotropic plate, the regions of parametric instability when expressed in non-dimensional form, are the same as those for the unstiffened flat plate.

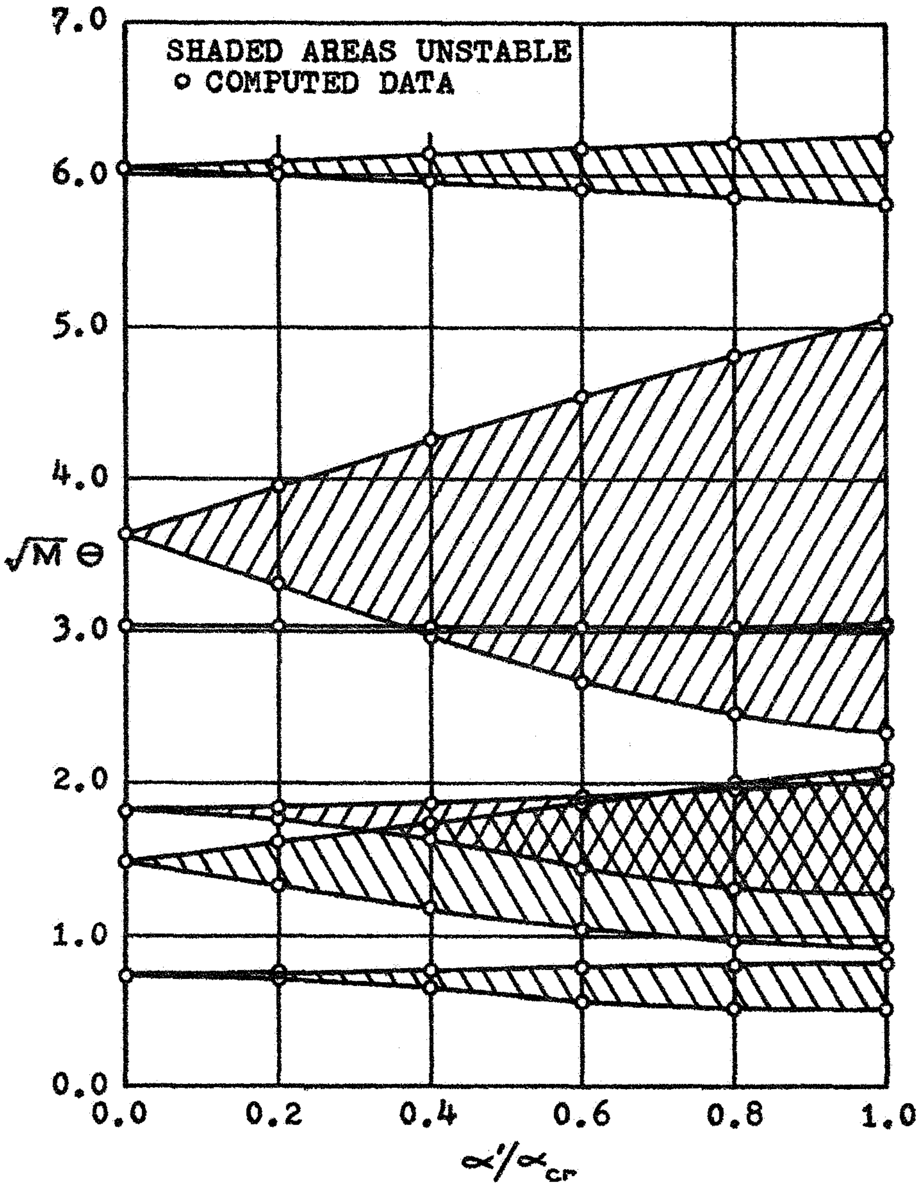

Fig. 16 Superposition of the First Spatial Modes

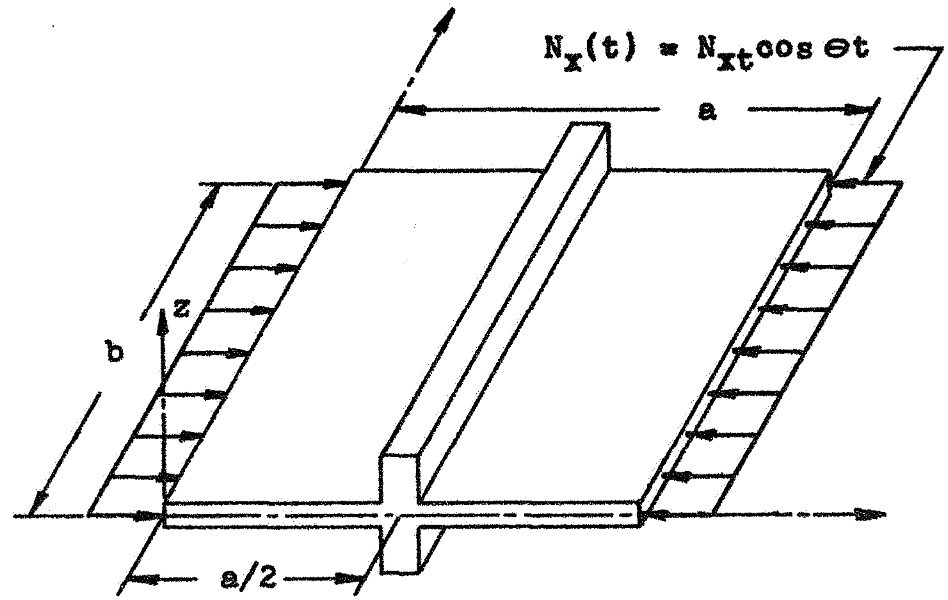

Beta = a/b = 1.0

$J_s = 1.0$

$\lambda_s = 0.2$

$N_{xo}/N_{xor} = 0.0$

Fig. 17 Stiffened Plate Configuration

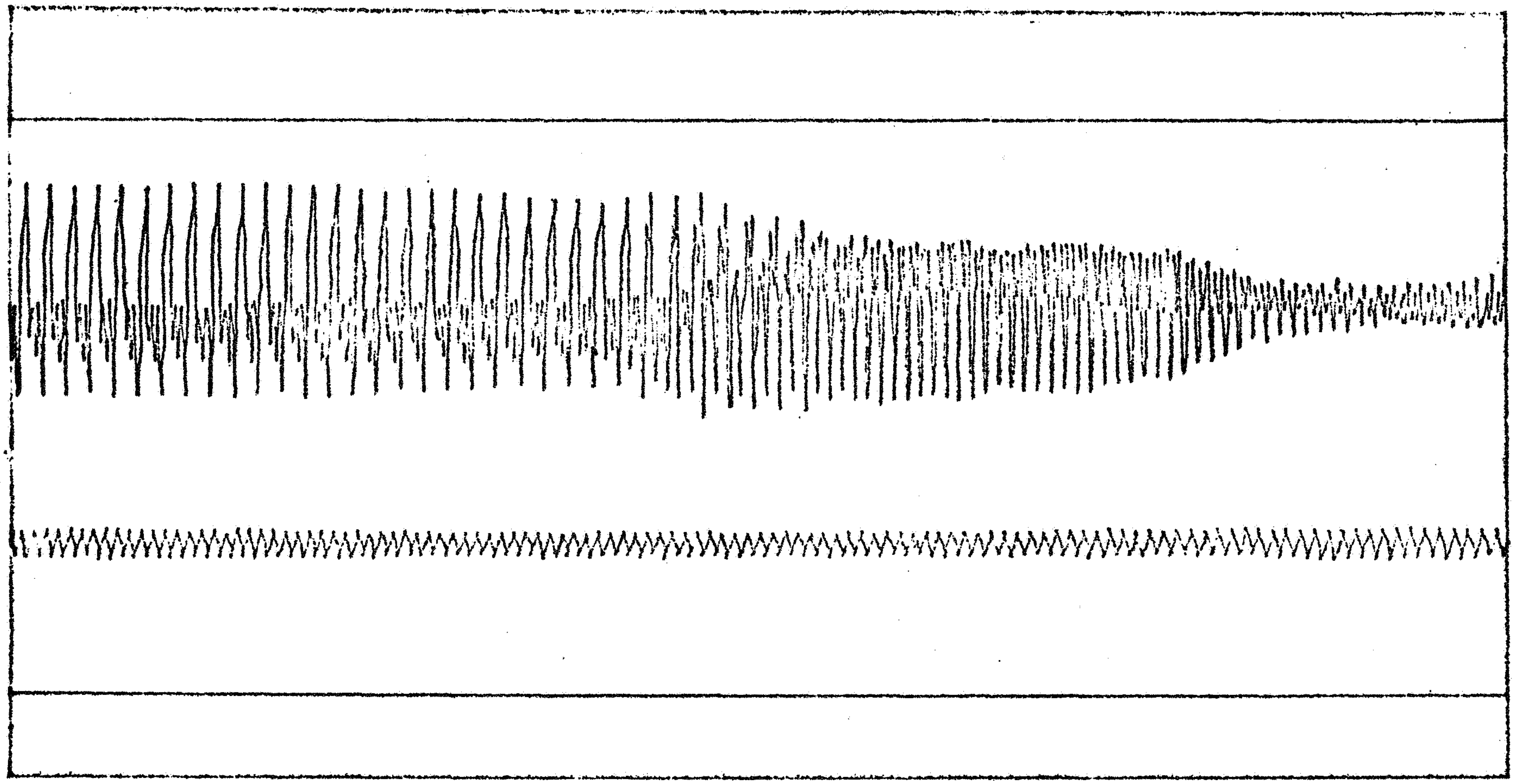

Fig. 18 Combined Motion Between the Principal Mode of the First Spatial Mode and the Second Temporal Mode Region of the Second Spatial Mode

4. CONCLUSIONS

Based on the results of this investigation the following conclusions can be drawn:

1. The theory developed in this investigation completely predicts the parametric response, natural frequencies and static buckling values for any simply-supported rectangular stiffened plate, with closely spaced stiffeners.

2. The most dangerous region of instability, from the standpoint of width, is the first temporal mode associated with the spatial mode which is the closest to the fundamental static stability mode.

3. The theories developed in this investigation only predict the boundaries of the regions of instability and they do not give information about the behavior of the stiffened plate within a region of instability.

4. The theory developed for the stiffened plate treated as an equivalent orthotropic model using the "smearing out" technique has a distinct advantage over the general orthotropic approach in that the stiffener size, spacing, and material properties are contained in the resulting expressions for the parametric response.

5. When the stiffened plate is analyzed as an equivalent orthotropic plate the regions of instability when expressed in nondimensional form, are the same as those for the unstiffened flat plate.

BIBLIOGRAPHY

1 Faraday, M. "On a Peculiar Class of Acoustical Figures, and on Certain Forms Assumed by a Group of Particles upon Vibrating Èlastic Surfaces," Phil. Trans. Roy. Soc., London, Vol. 121 (1831), 299-318.

2 Melde, F. "Uber Erregung Stehender Wellen eines fadenformigen Korpers," Ann. der Physik u Chemic, Vol. 109, Ser. 2 (1859), 193-215.

3 Strutt, J. W. (Lord Rayleigh). "On the Crispations of Fluid Resting upon a Vibrating Support," Phil. Mag., Vol. 16 (1883), 50-53.

4 Strutt, J. W. (Lord Rayleigh). "On the Maintenance of Vibrations by Forces of Double Frequency and on the Propagation of Waves through a Medium Endowed with a Periodic Structure," Phil. Mag., Vol. 24, Ser. 5 (1883). 145-159.

5 Beilin. E. A., and Dzhanelidze. "Survey of Work on the Dyanimc Stability of Elastic Systems," (in Russian), Prikl. Mat. i Mekhan., Vol. 16, No. 5 (1952), 635-648.

6 Evan-Iwanowski, R. M. "Parametric Instability of Elastic Systems," Developments in Theoretical and Applied Mechanics, Proceedings of the First Southeastern Conference on Theoretical and Applied Mechanics, Vol. I, Plenum Press, New York (1963), 100-109.

7 Evan-Iwanowski, R. M. "On the Parametric Response of Structures," Applied Mechanics Reviews, Vol. 18, No. 9 (1965), 699-702.

8 Beliaev, N. M. "Stability of Prismatic Rods Subject to Variable Longitudinal Forces," (in Russian), Collection of Papers: Engineering Constructions and Structural Mechanics (Inzhenernye sooruzhenilia i striotel' nais mekhanika), Leningrad, Put' (1924).

9 Weidenhammer, F. "Der Eingespante, Axial-Pulsierend Belastete Stabe als Stabilitat sproblem," Ingenieur Archiv., Vol. 19 (1951), 162-191.

10 Weidenhammer, F. "Nichtlineare Biegeschwingungen des Axial-Pulsierend Belasteten stabes, Ingenieur Archiv., Vol. 20 (1952), 315-330.

11 Bolotin, V. V. "On the Transverse Vibrations of Rods Excited by Periodic Longitudinal Forces," (in Russian), Collection of Papers: Transverse Vibrations and Critical Velocities, (Poperechnye Kolebaniia i Kriticheskie shorosti), Akademiia Nauk SSSR, Moscow, Vol. 1, 46-77.

12 Bolotin, V. V. "Determination of the Amplitudes of Transverse Vibrations Excited by Longitudinal Forces, (in Russian), Collection of Papers: Transverse Vibrations and Critical Velocities, (Poperechnye Koleboniia i kritcheskie shorosti), Akademiia Nauk SSSR, Moscow, Vol. 2, 45-64.

13 Grybos, R. "Parametric Vibration in a System with Non-Linear Characteristics," (in Polish), Rozprowy Inzynierskie, Vol. 14, No. 2 (1966), 215-230.

14 Utida, I. and K. Sezawa. "Dynamical Stability of a Column under Periodic Longitudinal Forces," Rep. Aeronaut. Res. Inst., Tokyo Imp. University, Vol. 15, No. 193 (1940), 139-183.

15 Somerset, J. H. "Parametric Instability of Elastic Columns," Syracuse University Research Institute Re-Report No. 1053-7 1962.

16 Somerset, J. H. and R. M. Evan-Iwanowski. "Experiments on the Parametric Instability of Columns," Developments in Theoretical and Applied Mechanics, Proceedings of the Second Southeastern Conference on Theoretical and Applied Mechanics, Vol. 2, Pergamon Press Ltd. (1965), 503-525.

17 Einaudi, R. "Sulle Configurazioni di Equilibrio Instabili di una Piastra Sollecitata de Sforzi Tangerziale Pulsanti," Atti Accad Gioenia, J. Memoria, Vol. 20, No. 1-5 (1935-1936).

18 Bolotin, V. V. The Dynamic Stability of Elastic Systems, English Translation, Holden Day, San Francisco (1964).

19 Bolotin, V. V. "Certain Nonlinear Problems of the Dynamic Stability of Plates," (in Russian), Izv. Adad. Nauk SSR, Otd. Tekhn. Nauk, Vol. 10, (1954) 47-59.

20 Somerset, J. H. "Large Amplitude Stabilization of Parametrically Excited Plate Vibration," Dissertation, Syracuse University (1965).

21 Somerset, J. H., and R.M. Evan-Iwanowski. "Experiments on the Large Amplitude Parametric Vibrations of Rectangular Plates," Developments in Theoretical and Applied Mechanics, Proceedings of the Third Southeastern Conference on Theoretical and Applied Mechanics, Vol. 3, Pergamon Press, Ltd., London (1966).

22 Somerset, J. H. "Transition Mechanisms Attendant to Large Amplitude Parametric Vibrations of Rectangular Plates," Presented at the A.S.M.E. vibration conference, Paper No. 67-Bibr-5 (1967).

23 Yu, Yi-Yuan, and Jai-Lue Lai. "Influence of Transverse Shear and Edge Conditions on Nonlinear Vibration and Dynamic Stability of Homogeneous and Sandwich Plates," Journal of Applied Mechanics, Transactions of the A.S.M.E., Vol. 33, No. 4 (1966), 934-936.

24 Yu, Ui-Yuan. "Application of Variation Equations of Motion to the Nonlinear Analysis of Dynamic Buckling," to be published in Proceedings of the Ninth Midwestern Mechanisms Conference.

25 Ambratsumyan, S. A., and V. T. Gnuni. "On the Dynamic Stability of Nonlinearly-Elastic Three-Layered Plates," (English Translation), Journal of Applied Mathematics and Mechanics, Vol. 25, No. 4 (1961), 1002-1108.

26 Ambratsumyan, S. A. and V. T. Gnuni. "On the Forced Vibration and Dynamic Stability of Three-Layered Orthotropic Plates," (in Russian), Izv, Akad. Nauk SSSR, Otd. Tekh. Nauk, Mekh. i Mash., No. 3 91961), 117-123.

27 Schmidt, G. "Nonlinear Parametric Vibration of Sandwich Plates," Proceeding of Vibration Problems, Vol. 6, No. 2 (1965), 209-228.

28 Ambratsumyan, S. A., and A. A. Khachaturian. "On the Stability and Vibrations of Anisotropic Plates," (in Russian), Dokladi Akad. Nauk Arm SSR, Vol. 29, No. 4 (1959), 159-166.

29 Ambratsumyan, S. A., and A. A. Khachaturian. "On the Stability of Vibrations of Anisotropic Plates,"(in Russian), Izv, Adad. Nauk SSSR, No. 1 (1960), 113-122.

30 Duffield, R. C., and N. Willems. "An Investigation of Dynamic Instability of Stiffened Rectangular Plates" Studies in Engineering Mechanics, Report No. 28, University of Kansas, Center for Research in Engineering Science, (1968).

31 Gerard, G. and Becker, H., "Handbook of Structural Stability, Part VII -- Strength of Thin Wing Construction," NASA TN D-162, 1959.

32 Siede, P., and Stein, M., "Compressive Buckling of Simply Supported Plates with Longitudinal Stiffeners," NACA TN 1825, 1949.

33 Wah, T., "Vibration of Stiffened Plates," The Aeronautical Quarterly, Vol. , No. , 1964, p. 285-289.

34 Hoppmann, W. H., "Bending of the Orthogonally Stiffened Plates," Journal of Applied Mechanics, Transaction of the A.S.M.E., Vol. , No. , 1955, p. 267-271.

35 Hoppmann, W. H., Huffington, N. J., and Magness, L. S., "Study of Orthogonally Stiffened Plates," Journal of Applied Mechanics, Transaction of the A,S,M.E., Vol. , No. , 1956, p. 343-350.

36 Hoppmann, W. H., "Elastic Compliances of Orthogonally Stiffened Plates," S.E.S.A. Proceedings, Vol. 14, No. 1, 137-144.

37 Beckett, R. E., "An Experimental Method for Determining the Elastic Constants of Orthogonally Stiffened Plates," Experimental Mechanics, Proceedings of the First International Congress on Experimental Mechanics, Pergamon Press, Ltd., London, (1963) 129-148.

38 Huffington, N. J., "Theoretical Determination of Rigidity Properties of Orthogonally Stiffened Plates," Journal of Applied Mechanics, Transaction of the A.S.M.E., Vol. . No. , (1956) 15-20.

39 Mikulas, M. M., and McElman, J. A., "On Free Vibrations of Eccentrically Stiffened Cylindrical Shells and Flat Plates," NASA 7N D-3010, (1965).

40 Black, D. L., Card, M. F., and Mikulas, M. M., "Buckling of Eccentrically Stiffened Orthotropic Cylinders," NASA TN D-2960, (1965).

41 Duffield, R. C. An Investigation of Parametric Stability of Stiffened Rectangular Plates, Dissertation, University of Kansas (1968).

42 Dettman, J. W., Mathematical Methods in Physics and Engineering, McGraw-Hill Book Company, Inc., New York, (1962).

43 Elsgolc, L. E., Calculus of Variations, Pergamon Press, Ltd. London, (1962).

44 Kantorovich, T. V., and Krylov, V. I., Approximate Methods of Higher Analysis, P. Noordhoff Ltd., Groningen, (1958).

45 Fung, Y. C., Foundations of Solid Mechanics, Prentice-Hall, Inc., Englewood Cliffs, N. J., (1965).

46 Lekhnitskii, S. G. Anisotropic Plates, OGIZ, Gostekhizdat, Moscow, (1947).

47 Courant, R., and Hilbert, D., Methods of Mathematic Physics, Interscience Publishers, Inc., New York, (1953) Vol. 1.

48 Coddingtion, E. A., and Levinson, N., Theory of Ordinary Differential Equations, McGraw-Hill Book Company, Inc., New York, (1955).

49 Thorkildsen, R. L. and Hoppmann, W. H. "Effect of Rotatory Inertia on the Frequencies of Vibration of Stiffened Plates," Journal of Applied Mechanics, Transactions of the A.S.M.E., Vol. 26, No. 2 (1959) 298-300.

50 Timoshenko, S. P., and Gere, J. M., Theory of Elastic Stability, McGraw-Hill Book Co., Inc., New York, (1961) 2nd Ed.

51 Francis, J. G. F. "The QR Transformation -- A Unitary Analogue to the LR Transformation," Computer Journal, Vol. 4, 265-271, 332-345.

52 Parlett, B. "The Development and Use of Methods of LR Type" STAM Review, Vol. 6, No. 3, 375-295.

53 Ralston, A. A First Course in Numerical Analysis, McGraw-Hill Book Company, Inc., New York, (1965).

54 Amad, F. P., and Yan Ness, J. E., "Eigenvalues by the QR Transform," Share Program Catalog, Program Description Submittal SDA No. 3006-01, August, 1964.

APPENDIX

Tables of Theoretical Results for the Orthotropic Model

(Mathieu's Equation)

P_t/P_{cr}		Temporal Mode 1		Temporal Mode 2		Temporal Mode 3		Temporal Mode 4	
		Upper	Lower	Upper	Lower	Upper	Lower	Upper	Lower
0.0	$\theta/2\Omega$	1.00000	1.00000	0.50000	0.50000	0.33333	0.33333	0.25000	0.25000
	$\theta^2/4\Omega^2$	1.00000	1.00000	0.25000	0.25000	0.11111	0.11111	0.06250	0.06250
0.2	$\theta/2\Omega$	1.09730	0.89900	0.50327	0.48338	0.33106	0.32764	0.24756	0.24683
	$\theta^2/4\Omega^2$	1.20407	0.80639	0.25328	0.23366	0.10960	0.10735	0.06128	0.06092
0.4	$\theta/2\Omega$	1.18897	0.79629	0.51242	0.43577	0.32869	0.30125	0.24260	0.23026
	$\theta^2/4\Omega^2$	1.41365	0.63407	0.26257	0.18989	0.10804	0.09075	0.05885	0.05302
0.6	$\theta/2\Omega$	1.27531	0.70921	0.52592	0.37944	0.32978	0.25959	0.23972	0.19755
	$\theta^2/4\Omega^2$	1.62641	0.50298	0.27659	0.14398	0.10876	0.06739	0.57467	0.03903
0.8	$\theta/2\Omega$	1.35689	0.65497	0.54221	0.35408	o.33463	0.24590	0.24087	0.18934
	$\theta^2/4\Omega^2$	1.84114	0.42899	0.29399	0.12537	0.11197	0.06047	0.05802	0.03585
1.0	$\theta/2\Omega$	1.43428	0.63305	0.56102	0.35119	0.34216	0.24678	0.24506	0.19099
	$\theta^2/4\Omega^2$	2.05716	0.40076	0.31374	0.12333	0.11707	0.06099	0.06006	0.03648
1.2	$\theta/2\Omega$	1.50800	0.65019	0.57877	0.35629	0.35130	0.25176	0.25101	0.19520
	$\theta^2/4\Omega^2$	2.27407	0.39714	0.33510	0.12694	0.12342	0.06338	0.06301	0.03811

Table 1 Theoretical Results Associated with Temporal Mode One Through Four

P_t / P_{cr}		Temporal Mode 5		Temporal Mode 6		Temporal Mode 7		Temporal Mode 8	
		Upper	Lower	Upper	Lower	Upper	Lower	Upper	Lower
0.0	$\theta/2\Omega$	0.20000	0.20000	0.16667	0.16667	0.14286	0.14286	0.12500	0.12500
	$\theta^2/4\Omega^2$	0.04000	0.40000	0.02778	0.02778	0.02041	0.02041	0.01563	0.01563
0.2	$\theta/2\Omega$	0.19791	0.19773	0.16490	0.16485	0.14134	0.14133	0.12368	0.12367
	$\theta^2/4\Omega^2$	0.03917	0.03910	0.02719	0.02718	0.01998	0.01997	0.01530	0.01530
0.4	$\theta/2\Omega$	0.19251	0.18626	0.15970	0.15630	0.13651	0.13455	0.11926	0.11808
	$\theta^2/4\Omega^2$	0.03706	0.03469	0.02550	0.02443	0.01864	0.01810	0.01422	0.01394
0.6	$\theta/2\Omega$	0.18809	0.15963	0.15464	0.13404	0.13123	0.11560	0.11394	0.10166
	$\theta^2/4\Omega^2$	0.03538	0.02548	0.02391	0.01797	0.01722	0.01336	0.01298	0.01034
0.8	$\theta/2\Omega$	0.18777	0.15427	0.15372	0.13028	0.13007	0.11275	0.11271	0.09946
	$\theta^2/4\Omega^2$	0.03526	0.02380	0.02363	0.01697	0.01692	0.01272	0.01270	0.00989
1.0	$\theta/2\Omega$	0.19060	0.15596	0.15586	0.13185	0.13182	0.11422	0.11421	0.10075
	$\theta^2/4\Omega^2$	0.03633	0.02432	0.02429	0.01738	0.01738	0.01305	0.01304	0.01015
1.2	$\theta/2\Omega$	0.19506	0.15951	0.15948	0.13489	0.13488	0.11686	0.11686	0.10309
	$\theta^2/4\Omega^2$	0.03805	0.02544	0.02544	0.01819	0.01819	0.01366	0.01366	0.01063

Table 2 Theoretical Results Associated with Temporal Mode Five Through Eight

P_t/P_{cr}		Temporal Mode 9		Temporal Mode 10		Temporal Mode 11		Temporal Mode 12	
		Upper	Lower	Upper	Lower	Upper	Lower	Upper	Lower
0.0	$\theta/2\Omega$	0.11111	0.11111	0.10000	0.10000	0.09091	0.09091	0.08333	0.08333
	$\theta^2/4\Omega^2$	0.01235	0.01235	0.01000	0.01000	0.00826	0.00826	0.00694	0.00694
0.2	$\theta/2\Omega$	0.10994	0.10994	0.09895	0.09895	0.08995	0.08995	0.08246	0.08246
	$\theta^2/4\Omega^2$	0.01209	0.01209	0.00979	0.00979	0.00809	0.00809	0.00680	0.00680
0.4	$\theta/2\Omega$	0.10588	0.10517	0.09523	0.09478	0.08653	0.08624	0.07930	0.07911
	$\theta^2/4\Omega^2$	0.01121	0.01106	0.00907	0.00898	0.00749	0.00744	0.00629	0.00626
0.6	$\theta/2\Omega$	0.10065	0.09076	0.09012	0.08199	0.08158	0.07478	0.07451	0.06874
	$\theta^2/4\Omega^2$	0.01013	0.00824	0.00812	0.00672	0.00666	0.00560	0.00556	0.00473
0.8	$\theta/2\Omega$	0.09943	0.08896	0.08895	0.08047	0.08047	0.07346	0.07346	0.06757
	$\theta^2/4\Omega^2$	0.00989	0.00791	0.00791	0.00648	0.00647	0.00540	0.00540	0.00457
1.0	$\theta/2\Omega$	0.10075	0.09013	0.09012	0.08153	0.08153	0.07443	0.07443	0.06847
	$\theta^2/4\Omega^2$	0.01015	0.00812	0.00812	0.00665	0.00665	0.00554	0.00554	0.00469
1.2	$\theta/2\Omega$	0.10309	0.92221	0.92221	0.08343	0.08343	0.76161	0.76166	0.07004
	$\theta^2/4\Omega^2$	0.01063	0.00850	0.00850	0.00696	0.00696	0.00580	0.00580	0.00491

Table 3 Theoretical Results Associated With Temporal Mode Nine Through Twelve

STUDIES IN ENGINEERING MECHANICS

1. "Vibration of Steel Joist-Concrete Slab Floor System--Part I," by Kenneth H. Lenzen and Joseph E. Keller, September, 1959.
2. "A Study of Flow Through Abrupt Expansions: Progress Report I, Mean Characteristics of Flow," by Neel Kanth D. Sharma, February, 1959.
3. "Vibration of Steel Joist-Concrete Slab Floor System--Part II," by Kenneth H. Lenzen and Joseph E. Keller, May, 1960.
4. "Damping Considerations in Vibration Response of Humans," by Joseph E. Keller, May, 1960.
5. "A Study of the Vibration of Rectangular Anisotropic Plates by the Ritz Method," by James A. Wiley, May, 1960.
6. "A Study of Flow Through Abrupt Expansions: Progress Report II, Pressure Fluctuations in Flow," by Charles L. Sanford and David W. Appel, June, 1961.
7. "A Study of Flow Through Abrupt Two-Dimensional Expansions: Progress Report III, Formation of Vortices," by Charles L. Sanford, June, 1961.
8. "A Study of the Dynamics of Flow Through Suction-Box Covers: Progress Report I, Flows Without Resistance," by Allen T. Hjelmfelt, June, 1961.
9. "Vibration Damping of Anisotropic Plates," by Gerald W. Barr, June, 1961.
10. "Stress in Unstiffened Cylindrical Shells Containing a Granular Material," by John T. Easley, June, 1961.
11. "A Study of the Dynamics of Flow Through Suction-Box Covers: Progress Report II, Flows with Resistance," by William H. Y. Lee, February, 1962.
12. "A Study of Various Damping Devices for Controlling Vibrating Floor Systems," by William C. Lyons, June, 1962.
13. "Characteristics of Flow Through Symmetrical Laterals: Progress Report I," by Carl T. Herakovich and John V. Otts, June 1, 1962.
14. "Separation of Flow at Interior Corners: Progress Report I, Geometry of Separation Zone," by Karl G. Maurer, June 1, 1962.
15. "A Study of Flow Through Abrupt Expansions: Progress Report IV, Effect of Gate Oscillation," by Svein Vigander, June, 1962.

16. "Vibration of Steel Joist-Concrete Slab Floor Systems: Final Report," by Kenneth H. Lenzen, August, 1962.

17. "Free-Streamline Analyses of Flow Nozzles, Flow through Side Inlets and Flow Past Corners," David W. Appel, March, 1963.

18. "Effect of Bearing Stresses on the Fatigue Strength of a Structural Joint," Tehyu Chu, May, 1966.

19. "Pilot Study--The Applicability of the AISC Formula to the Top Chords of Steel Joists," by Kenneth H. Lenzen, 1965.

20. "Separation of Laminar and Transitional Flows at an Interior Corner," by Mack H. Gray III, March, 1965.

21. "An Experimental Study of Wall-Pressure Fluctuations in a Cavitating Turbulent Shear Flow," by Svein Vigander, May, 1965.

22. "The Jayhawk Bender--A Structural Analysis Program," by J. B. Tiedemann, February, 1966.

22A. "Performance of Human Operators under Various System Parameters," by Hajime Akashi and Saad Mahmood, June, 1965.

23. "Computer Analysis of Two Dimensional Rigid Joint Frames," by V.S. Varadachary, June, 1966.

24. "Inelastic Behavior of the Compression Chord of Open-Web Steel Joists," by W. Scott McDonald, Jr., 1966.

25. "Uniform Load Testing of Open-Web Steel Joists," by Robert D. Ohmart, 1966.

26. "Vibrations in Floor Systems of Steel-Framed Buildings," by Leslie D. Meyer, May, 1967.

27. "Design Formulas for the Top Chords of Open-Web Steel Joists: Final Report," by Kenneth H. Lenzen, April, 1968.

28. "An Investigation of Parametric Stability of Stiffened Rectangular Plates," by Nicholas Willems and Roger C. Duffield, March, 1968.

29. "Vibration of Steel-Beam Concrete Slab Floor Systems," by Kenneth H. Lenzen and Thomas M. Murray, April, 1968.

30. "An Approximate Method for the Response of Stiffened Plates to Aperiodic Excitation," by Robert D. Ohmart, April, 1968.

31. "An Investigation of the Parametric Resonance of Rectangular Plates Reinforced with Closely Spaced Stiffeners," by Nicholas Willems and Roger C. Duffield, August, 1968.

CRES LABORATORIES

Chemical Engineering Low Temperature Laboratory

Remote Sensing Laboratory

Electronics Research Laboratory

Chemical Engineering Heat Transfer Laboratory

Nuclear Engineering Laboratory

Environmental Health Engineering Laboratory

Digital Computer Technology Laboratory

Water Resources Institute